

MOL#86744

## Title page

# Orexin-A Activates Hypothalamic AMPK Signaling through a Ca<sup>2+</sup>-dependent Mechanism Involving Voltage-gated L-type Calcium Channel

Wen-Ning Wu, Peng-Fei Wu, Jun Zhou, Xin-Lei Guan, Zui Zhang, Yuan-Jian Yang,  
Li-Hong Long, Na Xie, Jian-Guo Chen, Fang Wang

Department of Pharmacology, Tongji Medical College, Huazhong University of Science and Technology (HUST), Wuhan, Hubei 430030, China. (W.N.W, P.F.W, J.Z, X.L.G, Z.Z, Y.J.Y, L.H.L, N.X, J.G.C, F.W)

Key Laboratory of Neurological Diseases (HUST), Ministry of Education of China,  
The Key Laboratory for Drug Target Researches and Pharmacodynamic Evaluation of Hubei Province, Wuhan 430030, China. (P.F.W, L.H.L, N.X, J.G.C, F.W)

Department of Pharmacology, Anhui Medical University, Hefei, 230032, China  
(W.N.W)

MOL#86744

## Running Title Page

### Running Title:

L-type  $\text{Ca}^{2+}$  channel mediates hypothalamic AMPK activation

Corresponding Author Information:

Dr. Fang Wang,

Department of Pharmacology, Tongji Medical College, HUST, Wuhan, Hubei 430030,  
China

E-mail address: wangfangtj0322@163.com, Tel: +86 27 83692636, Fax: +86 27  
83692608

Number of text pages: 35

Number of figures: 7

Number of tables: 0

Number of references: 58

Number of words in the Abstract: 165

Number of words in the Introduction: 527

Number of words in the Discussion: 1352

**Abbreviations Used:** AMPK, AMP-activated protein kinase; Ara-A, 9-beta-D-arabinofuranoside; ARC, arcuate nucleus; CaMKKs, calmodulin-dependent protein kinase kinases;  $[\text{Ca}^{2+}]_i$ , cytosolic free  $\text{Ca}^{2+}$ ; DMEM, Dulbecco's Eagle's medium; i.c.v, intracerebroventricular; LHA, lateral hypothalamic area; NPY, neuropeptide Y; OX1R, OX1 receptor; PLC, phospholipase C; PKC, protein kinase C; POMC, proopiomelanocortin; VGCCs, voltage-gated calcium channels; TRPCs, transient receptor potential channels; TG, thapsigargin.

MOL#86744

## Abstract

Hypothalamic AMP-activated protein kinase (AMPK) and orexins/hypocretins are both involved in the control of feeding behavior, but little is known about the interaction between these two signaling systems. Here, we demonstrated that orexin-A elicited significantly activation of AMPK in the arcuate nucleus (ARC) of hypothalamus by elevating  $[Ca^{2+}]_i$  involving extracellular calcium influx. Electrophysiological results revealed that orexin-A increased L-type calcium current via orexin receptor-phospholipase C-protein kinase C (OXR-PLC-PKC) signaling pathway in ARC neurons that produce neuropeptide Y (NPY), an important downstream effector of orexin-A's orexigenic effect. Furthermore, L-type calcium channel inhibitor, nifedipine, attenuated orexin-A-induced AMPK activation *in vitro* and *in vivo*. We found that inhibition of AMPK by either compound C or the ATP mimetic 9-beta-D-arabinofuranoside (ara-A) prevented the appetite-stimulating effect of orexin-A. This action can be mimicked by nifedipine, the blocker of L-type calcium channel. Our results indicated that orexin-A activates hypothalamic AMPK signaling through a  $Ca^{2+}$ -dependent mechanism involving voltage-gated L-type calcium channel, which may serve as a potential target for regulating feeding behavior.

## Introduction

Hypothalamic neuronal circuits that respond to hunger or satiety signals control the drive to eat (Horvath and Diano, 2004; Pinto et al., 2004). To regulate the feeding behavior, orexigenic peptides such as neuropeptide Y (NPY), agouti-related protein (AgRP),  $\alpha$ -melanocyte stimulating hormone ( $\alpha$ -MSH) and orexins are secreted by neurons from different areas of the hypothalamus. Orexin-A, a neuropeptide with a stimulatory effect on feeding via the selective OX1 receptor (OX1R) (Edwards et al., 1999; Haynes et al., 2000; Sakurai et al., 1998; Yamada et al., 2000), is mainly secreted by the neurons in lateral hypothalamus area (LHA) that project far and wide in the hypothalamus, including the ARC (Date et al., 1999; de Lecea et al., 1998). It is well documented that orexin-A plays an important role in both normal energy homeostasis and abnormal control of eating behavior such as anorexia nervosa (Baranowska et al., 2008; Bronsky et al., 2011). NPY-containing neurons in the ARC, which have a strong orexigenic effect on feeding, have been shown to express orexin receptors and many evidence supports that NPYergic signaling mediates orexin-A's appetite-stimulating effect (Dube et al., 2000; Ida et al., 2000; Jain et al., 2000; Yamanaka et al., 2000). However, the precise molecular mechanism links OX1R with NPYergic function still remains largely unknown.

Recently, it has been revealed that hypothalamic AMP-activated protein kinase (AMPK) is a key sensor of energy status that underlies orexigenic effects of many hormones. For example, adiponectin increases food intake by activating AMPK in the arcuate hypothalamus (Kubota et al., 2007; Wen et al., 2010) and ghrelin promotes feeding through a mechanism involving the short-term activation of hypothalamic AMPK (Lopez et al., 2008). Accumulated evidence indicates that AMPK in NPY neurons senses hunger signal and shifts energy homeostasis toward increased food intake (Kohno et al., 2011; Murphy et al., 2009). For instance, decreased leptin and glucose after fasting activated AMPK in NPY-glucose-inhibited neurons and increased neurons excitation, which led to NPY release and food intake (Murphy et al., 2009). A novel finding has revealed that hunger signal results in a persistent

up-regulation of excitatory synaptic input to NPY neurons, then increases their firing rate via an AMPK-dependent positive feedback loop (Yang et al., 2011). Therefore, AMPK signaling in NPY neurons may be a common pathway that integrates orexigenic cues to control feeding behavior. AMPK can be indirectly activated by  $[Ca^{2+}]_i$  via  $Ca^{2+}$ -sensitive calmodulin-dependent protein kinase kinases (CaMKKs) (Anderson et al., 2008; Bair et al., 2009; Fogarty et al., 2010). It has been demonstrated that appetite-regulating hormones such as ghrelin and orexin-A increase  $[Ca^{2+}]_i$  in many native neurons, including NPY neurons (Kohlmeier et al., 2008; Uramura et al., 2001; Xu et al., 2002). Thus, calcium-dependent activation of AMPK may couple orexin-A's action with NPYergic system. Voltage-gated calcium channels (VGCCs) are the main route of calcium entry in neurons (Kohlmeier et al., 2008; Uramura et al., 2001; Xu et al., 2002). However, there are few reports about the role of VGCCs in AMPK activation. Here, we demonstrated for the first time that regulation of VGCCs by orexin-A stimulated AMPK activation in hypothalamic neurons. Furthermore, it was shown that VGCCs-dependent AMPK activation was also involved in orexin-A-mediated feeding behavior.

## Materials and Methods

**Chemicals** Orexin-A was purchased from Phoenix Pharmaceuticals (Burlingame, CA, USA). Anti-NPY serum H was obtained from Chemicon International (Temecula, CA, USA). SB334867 was purchased from Tocris (Bristol, UK). U73122, GF109203X, STO609, BayK8644, BAPTA-AM, EGTA, thapsigargin (TG), SKF96365, 9-beta-D-arabinofuranoside (ara-A) and nifedipine were obtained from Sigma (St. Louis, MO, USA), Compound C and B27 supplement were obtained from Gibco invitrogen Corporation (Carlsbad, CA, USA).  $\omega$ -conotoxin GVIA and  $\omega$ -agatoxin TK were obtained from Alomone labs (Jerusalem, Isreal). AMPK antibody and LKB1 antibody were obtained from Cell Signaling Technology. Other general agents were purchased from commercial suppliers. Orexin-A was prepared freshly with distilled water and others were dissolved in dimethylsulfoxide (DMSO) and stored at -20°C.

MOL#86744

They were diluted to the final concentrations before application. The final concentration of DMSO was <0.05%.

**I.c.v cannulation and injection** Male Sprague-Dawley rats weighing 250-300 g were housed at a controlled environment with temperature of  $22 \pm 1^{\circ}\text{C}$ , humidity of 70% and a 12 h-light/12 h-dark cycle from 08:00 to 20:00 h. Laboratory standard food and water were available ad libitum. Care of the rats was conducted according to the requirements of the ‘Guide for the Care and Use of Laboratory Animals’ by the National Research Council. The cannula was implanted according to Paxinos and Watson (Paxinos et al., 1980) with some modifications. Rats were anesthetized with 350 mg/kg chloral hydrate by intraperitoneal injection and placed in a stereotaxic apparatus with the bregma and posterior in the same level. The body temperature was maintained at  $37.0 \pm 0.2^{\circ}\text{C}$  by an electric incandescent lamp. In order to fix the cannula, three small holes were drilled into the bone to place a jeweler screw. A forth hole was made to insert a cannula into the lateral ventricle (LV, 0.8 mm posterior to the bregma, 1.4 mm lateral to the midline, 3.5 mm from the cranial theca). A stainless steel cannula with 7 mm long and 0.6 mm OD was implanted into the place according to the coordinates located above. The cannulae were fixed to the skull with the aid of jeweler screws and dental acrylic resin skull and cranioplastic dental cement. To maintain patency, a stylus 0.5 mm longer than the guide cannula was inserted into the guide. Cannula placement was confirmed by injection of black ink. The experiments were begun after a 7-day recovery period from surgery. After removal of the stylus from cannula, the drugs were injected into the lateral ventricle with a microsyringe ( $10\mu\text{L}$ ) connected by a PE-10 polyethylene tubing (10 cm) to a needle (OD=0.3 mm), 0.5 mm longer than guide cannula, which was introduced into the brain through the cannula fixed to the head of rat. The injection volume was set to  $5\mu\text{L}$  within a period of 5-10 min.

**Western blotting** After treatment, animals were sacrificed by decapitation under 10% chloral hydrate anesthesia and entire ARC tissue was isolated from brain slice. Culture

MOL#86744

cell or isolated ARC tissue was washed twice with ice-cold PBS and then lysed on ice in extraction buffer containing 50 mM Tris-base (pH 7.4), 100 mM NaCl, 1% NP-40, 10 mM EDTA, 20 mM NaF, 1 mM PMSF, 3 mM Na<sub>3</sub>VO<sub>4</sub> and protease inhibitors. The homogenates were centrifuged at 12,000 g for 15 min at 4 °C. Supernatant was separated and stored at -80 °C until use. Protein concentration was determined using the BCA protein assay kit (Pierce Biotechnology, Inc., Rockford, IL, USA). Protein samples (30µg) were separated by 10% SDS-polyacrylamide gel and then transferred to nitrocellulose membranes. After blocking with 5% nonfat milk in Tris-buffered saline containing 0.1% Tween-20 (TBST) for 1 h at room temperature, transferred membranes were incubated overnight at 4 °C with different primary antibodies (phospho-AMPK and AMPK 1:800 dilution; phospho-LKB1 and LKB1 1:800 dilution;). Following three washes with TBST, membranes were then incubated with horseradish peroxidase-conjugated secondary antibodies (1:3000) in TBST with 1% nonfat milk for 1 h at room temperature. After repeated washes, membranes were reacted with enhanced chemiluminescence reagents (Amersham Pharmacia Biotech, Inc., Piscataway, NJ, USA) for 5 min, and visualized with X-ray films (Kodak X-Omat, Rochester, NY, USA). The films were scanned and the optical density of the bands was determined using Optiquant software (Packard Instrument). Results are expressed as percentage of control signals (% control) in each blot to correct for variations between blots.

**Assay of AMP /ATP ratio** The procedure for assay of AMP /ATP ratio in the ARC of male SD rats was executed as that described by Coolen et al with some modifications (Coolen et al., 2008). Samples dissected from ARC were homogenized and vortex mixed for 5 min with 0.5 mL of ice-cold 8% perchloric acid (v/v) in a 1.5 mL Eppendorf tube. After precipitation of the protein fraction (at 12000 g, 10 min, 4 °C), the supernatant was removed and neutralized to pH 6.5 with 0.65 mL of 6 M KOH and 40µL of 2 M K<sub>2</sub>CO<sub>3</sub>. The mixture was vortex mixed and centrifuged for 5min, and the supernatant was collected in a 5 mL test tube. The volume was made up to 5 mL with 0.05 M NH<sub>4</sub>H<sub>2</sub>PO<sub>4</sub> (pH 5.70). A sample from the solution was drawn into a

MOL#86744

pipette and filtered through a filtering cartridge with a 0.45 $\mu$ m nylon membrane using a disposable syringe set before HPLC analysis. A Thermo Finnigan HPLC system (ThermoFinnigan Corporation, San Jose, CA, USA) containing a Surveyor MS pump, a Surveyor PDA detector, an auto sampler and the Xcalibur TM 1.3 software. A reversed phase column (Agilent TC-C18, 250 $\times$ 4.6 mm, 5 $\mu$ m), kept at 30 °C, was also used. The standards and samples were separated using a gradient mobile phase consisting of 0.05 M NH<sub>4</sub>H<sub>2</sub>PO<sub>4</sub> (pH 5.7, A) and acetonitrile/water (60:40, v/v, B). The linear gradient conditions were as follows: 0-6.5 min, 100% A; 6.5-12.5 min, 100% B; 12.5-25 min, 100% A. The flow rate was set at 0.8 mL·min<sup>-1</sup>, and the injection volume was 20 $\mu$ L. The detection wavelength was set at 257 nm.

**Preparation of cultured neurons from ARC** All experiments conformed to local and international guidelines for the use of animals and all experimental protocols were approved by the Review Committee for the Use of Human or Animal Subjects of Huazhong University of Science and Technology. Primary cultures of ARC neurons were prepared as previously described (Muroya et al., 2004; Wang et al., 2008) with some modifications. Brains slices containing the entire ARC were prepared from the brains of neonatal Sprague-Dawley rats (day 2-3), and the entire ARC was excised from the left and right sides. The dissected tissues were treated with 0.125% trypsin in Hanks' balanced salt solution for 25 min at 37 °C and mechanically dissociated using a fire-polished Pasteur pipettes. Cells suspension was centrifuged for 7 min at 800 g and the cell pellets were resuspended in the modified Dulbecco's Eagle's medium (DMEM) and F-12 supplement (1:1) with 10% fetal bovine serum. For whole-cell patch-clamp recording, cells (20,000-40,000) were seeded on poly-D-lysine coated coverslips and kept at 37 °C in 5% CO<sub>2</sub> incubator. After 24 h, the culture medium was changed to DMEM medium supplemented with 2% B27 and the ARC neurons were fed with fresh medium twice weekly. Microscopically, glial cells were not apparent in ARC neurons cultures employing this protocol. The neurons were maintained for 7-10 d in primary culture until used for experiments.

MOL#86744

**Immunocytochemical identification of single ARC neurons** Single ARC neurons were immunocytochemically identified as previously reported with slight modifications (Muroya et al., 2004; Wang et al., 2008). In the voltage-clamp experiments, the cells with typical characteristics of NPY-positive neurons were selected to record, photograph to mark position and sequence. Then the cells were fixed with 4% paraformaldehyde in 0.1 M PBS overnight. They were pretreated with H<sub>2</sub>O<sub>2</sub> in methanol for 1 h. Nonspecific binding sites were then blocked with 10% goat serum in 0.1 M PBS for 1 h at room temperature. Cells were incubated overnight at 4 °C with primary antiserum to NPY diluted 1:1,000 in PBS containing 1.5% normal goat serum. Cells were subsequently incubated with biotinylated goat anti-rabbit IgG secondary antibody for 1 h at room temperature. The secondary antibody was then rinsed, and the sections were labeled with avidin-peroxidase complex reagent (ABC kit; Vector) for 1 h. The sections were developed with 3,3'-diaminobenzidine. In control sections, the primary antibodies were replaced by the corresponding nonspecific IgG and processed in parallel.

**Whole-cell patch-clamp recording** The procedure for whole-cell patch-clamp recording was executed as that described in our previous reports with minor modification (Ma et al., 2009; Wang et al., 2008). The bath solution for recording high-voltage activated calcium current ( $I_{HVA}$ ) contained (in mmol/L): Choline-Cl 110, MgCl<sub>2</sub> 2, CaCl<sub>2</sub> 10, TEA-Cl 20, HEPES 10, Glucose 10, and the pH was adjusted to 7.4 with CsOH. Glass pipettes were used with a resistance of about 2-4 MΩ when filled with the following solution (in mmol/L): CsF 64, CsCl 64, CaCl<sub>2</sub> 0.1, MgCl<sub>2</sub> 2, EGTA 10.0, HEPES 10.0, Tris-ATP 5.0, and the pH was adjusted to 7.2 with CsOH. After establishing a whole-cell configuration (Date et al., 1999), the adjustment of capacitance compensation and series resistance compensation was done before recording. The current signals were acquired at a sampling rate of 10 kHz and filtered at 3 kHz. Whole-cell patch-clamp recordings were carried out using an EPC-10 amplifier (HEKA, Lambrecht, Germany) driven by Pulse/PulseFit software (HEKA, Southboro, Germany). Drug actions were measured only after steady-state conditions

MOL#86744

reached, which were judged by the amplitudes and time courses of currents remaining constant. All the recordings were made at room temperature (20-22 °C). All experiments were repeated three times using different batches of cells and at least the 3-4 dishes with cells were used for recording in different batches of cells.

**Calcium imaging** Digital calcium imaging was performed as described by Ming et al (Lin *et al.*, 2007; Ming *et al.*, 2006). The cells were washed three times by artificial cerebrospinal fluid (ACSF) containing (in mM): 140 NaCl, 5 KCl, 1 MgCl<sub>2</sub>, 2 CaCl<sub>2</sub>, 10 glucose, and 10 HEPES (pH 7.3), then loaded with 1 μM Fura-2/AM in ACSF for 30 min at 37 °C to remove the excess extracellular Fura-2/AM. Coverslips were then mounted on a chamber positioned on the movable stage of an inverted microscope (TE2000, Japan), which was equipped with a calcium imaging system (PTI, USA). The cells were superfused by ACSF at a rate of 2 ml/min for 10 min. Fluorescence was excited at wavelengths of 340 nm for 150 ms and 380 nm for 50 ms at 1 s interval by a monochromator (PTI K-178-S) and the emission was imaged at 510 nm with a video camera (CoolSNAP HQ2, ROPPER, USA) through fluor oil-immersion lens (Nikon) and a wide band emission filter. F340/F380 fluorescence ratio was recorded and analyzed by MetaFluor version 6.3 software. In each experiment, the peak 340/380 ratio after addition of control solution or orexin was averaged in the graphs. The control means the 340/380 ratio after addition of control solution. Then, on the same cell, the peak 340/380 ratio after addition of orexin was measured and averaged. All experiments were repeated at least three times using different batches of cells to ensure reproducibility.

**Feeding study** Firstly, the effect of drugs (Compound C, ara-A, nifedipine, STO609 and U73122) on orexin-A-mediated feeding was investigated in *ad libitum* fed rats. Orexin-A was prepared freshly with distilled water and others were dissolved in DMSO. Before injection, the final concentration of DMSO was set at 0.5%. The male SD rats were divided into vehicle group (distilled water), orexin-A group and other drugs combined with orexin-A group. Cumulative food intakes were measured at 1, 2

MOL#86744

and 4 h after injection of the drugs into the lateral ventricle by the cannula. All of the experiments of feeding behavior were conducted in the light of early phrase. To test the effect of nifedipine on re-feeding after fasting, all experimental rats were fasted (with free access to water) for 24 h before being injected with nifedipine or vehicle (DMSO). 15 min after injection, rats were given ad libitum access to food, and cumulative food intakes were measured at 1, 2 and 4 h after re-feeding.

**Measurement of NPY content** The procedure for NPY analysis was executed as that described by Rocha et al with minor medications (Rocha et al., 2006). After treatment, animals (male SD rats) were sacrificed by decapitation under 10% chloral hydrate anesthesia and entire ARC tissue was isolated from brain slice. Culture cell or isolated ARC tissue was washed twice with ice-cold PBS and then lysed on ice in extraction buffer containing 50 mM Tris-base (pH 7.4), 100 mM NaCl, 1% NP-40, 10 mM EDTA, 20 mM NaF, 1 mM PMSF, 3 mM Na<sub>3</sub>VO<sub>4</sub> and protease inhibitors. The homogenates were centrifuged at 12,000 g for 15 min at 4°C. Supernatant was separated and stored at -80°C until use. Protein concentration was determined by using the BCA protein assay kit (Pierce Biotechnology, Inc., Rockford, IL, USA) and NPY content was measured by a commercial enzyme linked immunosorbent assay (ELISA) kit (R&D, USA) according to the manufacturer's protocol. NPY content was expressed as pg/μg protein.

**Electrophysiological data analysis** Only the results from NPY-immunoreactive neurons were collected into data statistics. Dose-response curve was fitted with the Hill equation:  $I/I_{max}=1/[1+(EC_{50}/C)^n]$ , where I is the current amplitude after administration of orexin A  $I_{max}$  is the control current amplitude, C is the concentration of orexin A itude, and n is Hill coefficient. The voltage-dependence of activation was determined using standard protocols. The conductance G was calculated according to  $G=I/(V_m-V_{rev})$ , where  $V_{rev}$  is the Ca<sup>2+</sup> reversal potential and  $V_m$  is the membrane potential at which the current was recorded. Normalized peak conductance ( $G/G_{max}$ ) was then fitted by the following Boltzmann equation:  $G/G_{max}=$

$1/\{1+\exp[(V_{1/2}-Vm)/k]\}$ , where  $G_{max}$  is the maximum conductance,  $V_{1/2}$  is the membrane potential of half-maximal activation, and  $k$  indicates the slope factor. To investigate the voltage-dependent inactivation, normalized currents ( $I/I_{max}$ ) were plotted against the voltages of conditioning voltage, and fitted with a Boltzmann function:  $I/I_{max}=1/\{1+\exp[(V_{1/2}-Vm)/k]\}$ , where  $I_{max}$  is the maximal current,  $V_m$  is the conditioning voltage,  $V_{1/2}$  is the potential of half-maximal inactivation and  $k$  is the slope factor.

**Statistical analysis** Values were presented as mean  $\pm$  S.E.M. Data from experiments were analyzed with the statistical program SPSS (SPSS, Chicago, IL, USA). A two-sided Student's t-test with paired comparisons was used to evaluate differences of electrophysiological data. For other data, comparison between two groups was evaluated by a two-sided and unpaired Student's t-test. Comparison between three or four groups was evaluated by ANOVAs and post-hoc tests. One-way ANOVA with repeated measures followed by Student's t-test were used to analyze the data of food intake between groups at every test time point respectively. Differences at the  $p < 0.05$  level were considered statistically significant.

## Results

### Orexin-A activates AMPK via CaMKK $\beta$ -dependent pathway in the rat hypothalamic ARC.

To test the effect of orexin-A on hypothalamic AMPK activation under an orexigenic condition, the AMPK phosphorylation in the ARC was tested at 0.5 h after injection of orexin-A (1 nmol). As shown in Fig. 1A, orexin-A significantly increased the phosphorylation of AMPK by  $69.67 \pm 19.13\%$ . We found that orexin-A did not change AMP/ATP ratio in the ARC (Fig. 1B) and it had no effect on phosphorylation of LKB1, an upstream AMPK kinase (Fig. 1C). Calmodulin-dependent protein kinase kinase  $\beta$  (CaMKK $\beta$ ) is one of the major types of calmodulin-dependent protein kinases (CaMKs) and activates AMPK (Anderson et al., 2008; Bair et al., 2009;

Fogarty et al., 2010). STO609 is widely used to inhibit CaMKK $\beta$  (Anderson et al., 2008; Pfisterer et al., 2011; Tokumitsu et al., 2003). I.c.v injection of STO609 inhibited AMPK activation induced by orexin-A in hypothalamic ARC (Fig. 1D), but had no effect on the phosphorylation of AMPK in hypothalamic ARC when used alone (Supplemental Fig. 1). These results suggest that under an orexigenic condition, orexin-A regulates AMPK via CaMKK $\beta$  activation in the hypothalamic ARC.

**Orexin-A stimulates AMPK activation via extracellular calcium-dependent pathway in the cultured rat ARC neurons.**

Previous studies show CaMKK $\beta$  is activated by  $\text{Ca}^{2+}$ /calmodulin and orexin-A increase  $[\text{Ca}^{2+}]_i$  in NPY neurons of ARC (Muroya et al., 2004). To further investigate the precise mechanism involved in the hypothalamic AMPK activation, cultured ARC neurons were used. According to the results of preliminary experiment (Supplemental Fig. 2), 100 nM orexin-A was selected to observe its effect in cultured ARC neurons. After 0.5 h, the phosphorylation of AMPK was increased significantly by  $82.64 \pm 22.76\%$  in ARC neurons (Fig. 2A). This effect was attenuated by the intracellular calcium chelator BAPTA-AM ( $10\mu\text{M}$ ), while BAPTA-AM alone exhibited little effect on AMPK activation in ARC neurons (Fig. 2B). These results indicate that orexin-A-mediated hypothalamic AMPK activation is calcium-dependent. Then, we further examined whether extracellular calcium influx or intracellular calcium release involved orexin-A-induced AMPK activation in ARC neurons. Firstly, the effect of orexin-A on AMPK activation in  $\text{Ca}^{2+}$ -free medium was observed. Pre-incubation with a slow  $\text{Ca}^{2+}$  chelator EGTA (5 mM) for 30 min alone had no effect on the activation of AMPK in ARC neurons, but it completely prevented orexin-A-induced AMPK activation (Fig. 2C). Secondly, the effect of intracellular calcium release on orexin-A-induced AMPK activation was investigated. Pre-incubation with a sarcoplasmic/endoplasmic reticulum (ER)  $\text{Ca}^{2+}$ -ATPase inhibitor TG for 30 min did not influence the activation of AMPK in ARC neurons. Interestingly, after depleting the intracellular calcium store by TG, orexin-A also induced AMPK activation in hypothalamic neuron (Fig. 2D), although this effect seemed to be partially attenuated.

These results suggest that extracellular calcium influx is predominant in orexin-A-induced AMPK activation in hypothalamic neurons, while  $\text{Ca}^{2+}$  release from intracellular store is also involved in this effect. We further confirmed this result by calcium imaging experiment. Orexin-A markedly increased  $[\text{Ca}^{2+}]_i$  by  $51.16 \pm 7.58\%$  in the ARC neurons. About  $59\% \pm 8.2\%$  of the ARC neurons can response to orexin-A, which was similar to the percentage of NPY-positive neurons ( $57\% \pm 6.4\%$ ). This effect was significantly attenuated in  $\text{Ca}^{2+}$ -free medium (Fig. 2E-F).

### **Orexin-A increases high-voltage activated calcium current ( $I_{\text{HVA}}$ ) in NPY neurons of ARC.**

Previous reports have suggested that VGCCs provide an important pathway for orexin-A-induced calcium signal (Kohlmeier et al., 2008; Uramura et al., 2001; Xu et al., 2002). Therefore, the effect of orexin-A on VGCCs was investigated in cultured rat hypothalamic NPY neurons, which are involved in orexin-A's orexigenic effect. As shown in Fig. 3A, NPY neurons are typically small and medium neurons with triangular or spindle-shaped perikaryons and poorly ramified primary dendrites. The percentage of NPY-positive neurons was about  $57\pm6.4\%$  in ARC neurons. In the voltage-clamp experiments, the cells with typical characteristics of NPY neurons were selected to record, photograph and sequence. After whole-cell patch-clamp recording, the cells were immunocytochemically identified as our previous reports (Wang et al., 2008; Yang et al., 2010). The cells were stepped from the holding potential of -80 mV to -40 mV (50 ms), and then depolarized to +10 mV (200 ms) after briefly hyperpolarizing the membrane potential for 10 ms to -45 mV (Fig. 3C). The  $I_{\text{HVA}}$  was activated by the second depolarization. The protocol was applied every 5 s. Among 34 neurons with characteristics of NPY neurons that responded to orexin-A, 30 neurons (88%) were proved to be NPY-immunoreactive neurons (Fig. 3B). Orexin-A (1 nM) increased the amplitude of  $I_{\text{HVA}}$  by  $31.28 \pm 2.80\%$ , and almost returned toward control level after washout (Fig. 3C). The concentration of orexin-A producing 50% increase in  $I_{\text{HVA}}$  ( $\text{EC}_{50}$ ) was  $0.75 \pm 0.09$  nM, and the Hill coefficient was  $0.72 \pm 0.19$  (Fig. 3D). The effect was observed 30-60 s after application of orexin-A, and rapidly reached a plateau in 90-150 s (Fig. 3E). To study the effect of orexin-A on the activation curve

of  $I_{HVA}$ , the currents were evoked by a series of 200 ms voltage steps between -50 mV and +50 mV in 10 mV increments preceded by the holding potential of -80 mV. The I-V curves in Fig. 3F indicated that the amplitude of  $I_{HVA}$  was voltage-dependent. Orexin-A at 1 nM increased the peak amplitude of  $I_{HVA}$  in NPY neurons, but had no effect on the reversal potential of  $I_{HVA}$ . At +10 mV, the current amplitude was increased from  $238 \pm 65$  pA to  $316 \pm 52$  pA in the presence of 1 nM orexin-A. As shown in Fig. 3G, 1 nM orexin-A shifted the activation curve of  $I_{HVA}$  positively with  $V_{1/2}=6.90 \pm 2.70$  mV,  $k=6.40 \pm 2.13$  in control group, and  $V_{1/2}=1.47 \pm 0.67$  mV,  $k=6.54 \pm 1.30$  by 1 nM orexin-A ( $P<0.05$ ). To investigate the steady-state inactivation properties of  $I_{HVA}$ , 300 ms conditioning prepulses from -90 mV to 20 mV in 10 mV increments were applied before step depolarizations to the fixed potential of 10 mV. Orexin-A at 1 nM did not significantly alter the voltage-dependence of inactivation kinetics of  $I_{HVA}$  in NPY neurons, with  $V_{1/2}=-36.34 \pm 7.50$  mV,  $k=-40.8 \pm 4.00$  in control group, and  $V_{1/2}=-30.36 \pm 5.98$  mV,  $k=-33.00 \pm 3.80$  in orexin-A group (Fig. 3H). In addition, we further observed that orexin-A can increase the frequency of action potentials and cause membrane depolarization in hypothalamic NPY neurons (Supplemental Fig.3), which may facilitate activation of VGCCs under basal conditions.

### Orexin-A mainly increases L-type calcium current via OX1R-PLC-PKC signaling pathway.

To further examine which type of calcium channel was regulated by orexin-A, the effects of orexin-A on  $I_{HVA}$  in these neurons were observed in the presence of nifedipine (L-type calcium channel blocker),  $\omega$ -conotoxin GVIA (N-type calcium channel blocker) and  $\omega$ -agatoxin TK (P/Q-type calcium channel blocker), respectively. As shown in Fig. 4A, after pre-treatment with 10 $\mu$ M nifedipine, orexin-A failed to increase the current amplitude of  $I_{HVA}$  in NPY neurons. However,  $\omega$ -conotoxin GVIA (1 $\mu$ M) and  $\omega$ -agatoxin TK (200 nM) did not affect orexin-A-induced  $I_{HVA}$  increase in NPY neurons (Fig. 4B-C), suggesting that L-type calcium channel mediates the effect of orexin-A on  $I_{HVA}$ . This point was confirmed by PCR. We found that both Cav1.2

MOL#86744

and Cav1.3 channel expressed in ARC neurons (Supplemental Fig.4). Previous reports have shown that activation of OX<sub>1</sub>R-PLC-PKC signaling pathway contributes to orexin-A-mediated [Ca<sup>2+</sup>]<sub>i</sub> elevation (Uramura et al., 2001). To determine whether the OX<sub>1</sub>R-PLC-PKC signaling pathway was involved in the effect of orexin-A on L-type calcium current, we employed SB334867 (selective OX<sub>1</sub>R antagonist), U73122 (PLC inhibitor) and GF109203X (PKC inhibitor) in this experiment. Application with SB334867, U73122 and GF109203X alone exhibited no effects on I<sub>HVA</sub>, but 10μM SB334867, U73122 and GF109203X significantly inhibited the increase in I<sub>HVA</sub> produced by orexin-A (Fig. 4D-F). These results suggest that L-type calcium channel and OXR1-PLC-PKC signaling pathway are required for orexin-A-induced upregulation of VGCCs function in hypothalamic NPY neurons.

### **L-type calcium channel mediates orexin-A-induced AMPK activation in hypothalamic ARC.**

Next, we further determined whether L-type calcium channel was involved in calcium-dependent AMPK activation induced by orexin-A in hypothalamic ARC. Firstly, Bay K 8644, a selective L-type calcium channel activator that prolongs Ca<sup>2+</sup> channel open times and elevates cytosolic Ca<sup>2+</sup> via L-type Ca<sup>2+</sup> channel under basal conditions (Dessy and Godfraind, 1996; Miyauchi et al., 1990; Mulvaney et al., 1999; Peti-Peterdi and Bell, 1999), was used to investigate the role of L-type calcium channel in AMPK activation. As shown in Fig. 5A, BayK8644 (10μM) promoted AMPK activation in the hypothalamic neurons and this effect can be inhibited by 10 μM STO 609, indicating that upregulation of L-type calcium channel function can lead to AMPK activation. Then, the effect of L-type calcium channel blocker nifedipine on orexin-A-induced AMPK activation was investigated. Pre-incubation with nifedipine (10μM) in cultured ARC neurons or i.c.v. injection of nifedipine (50 μg/kg) exhibited little effect on the hypothalamic AMPK activation, but largely inhibited orexin-A-induced AMPK activation (Fig. 5B-C). Considering that activation of PLC-PKC signaling pathway is responsible for the action of orexin-A on L-type calcium channel, we further investigated the effect of PLC-PKC signaling pathway on

MOL#86744

orexin-A-mediated hypothalamic AMPK activation. I.c.v injection of PLC inhibitor U73122 (10 nmol) had no effect on hypothalamic AMPK phosphorylation (data not shown), but reduced orexin-A-mediated hypothalamic AMPK activation (Fig. 5D). In our preliminary experiment, it was found that low concentration of orexin-A (1 nM) that can increase L-type calcium current exhibited little effect on AMPK activation (supplemental Fig. 2). Thus, besides VGCCs, there may exist other mechanisms. Orexin-A can also activate transient receptor potential cation channels (TRPCs). We found that i.c.v injection of SKF96365 (25 nmol), a blocker of TRPCs, partially attenuated but not abolished orexin-A-induced AMPK activation (Supplemental Fig. 5). These results suggest that although other calcium entry routes exist, L-type calcium channel is largely predominant in orexin-A-mediated hypothalamic AMPK activation.

**Calcium-dependent hypothalamic AMPK activation is involved in orexin-A-mediated NPY increase and feeding behavior.**

Hypothalamic AMPK signal is involved in the orexigenic signaling of metabolic hormones, including adiponectin and ghrelin. NPY, an important orexigenic peptide that secreted by NPY neurons, is considered as the downstream effector of orexin-A's orexigenic effects. Therefore, we further investigated the effect of hypothalamic AMPK on NPY content and feeding behavior induced by orexin-A. As shown in Fig. 6A-C, compared to the vehicle group, i.c.v injection of orexin-A (1 nmol) significantly increased NPY content in hypothalamic ARC. I.c.v injection of AMPK inhibitor compound C, CaMKK $\beta$  inhibitor STO609 and nifedipine inhibited the increase in NPY content induced by orexin-A, but exhibited little effect on hypothalamic NPY content when used alone, indicating that orexin-A increases hypothalamic NPY content via calcium-dependent AMPK activation.

Then, we determined the role of hypothalamic AMPK in orexin-A-induced feeding behavior. All of the drugs were dissolved in DMSO and we found i.c.v injection of DMSO (0.5%) exhibits little effect on orexin-A (Supplemental Fig.6). AMPK inhibitor compound C (500 nmol) significantly attenuated orexin-A stimulated

feeding behavior (Fig. 6D), while it did not influence the feeding behavior at 1 h and 2 h after i.c.v. injection and slightly inhibited food intake at 4 h after i.c.v. injection. Considering that compound C has been shown to block other protein kinases with similar potency, the ATP mimetic ara-A, a precursor of ara-ATP that can decrease the AMP: ATP ratio within cells and inhibit AMPK activation (Potter et al., 2010; Russell et al., 1999; Wu et al., 2003), was used as an AMPK inhibitor to confirm the role of AMPK in orexin-A-induced food intake. Similarly, i.c.v. injection of ara-A (2 $\mu$ mol) did not influence the feeding behavior, but significantly inhibited orexin-A-induced food intake (Fig. 6E). Then, inhibitors of AMPK upstream kinases such as CaMKK $\beta$  inhibitor STO609 and PLC inhibitor U73122 were also used. Both STO609 and U73122 exhibited little effect on food intake, but they inhibited orexin-A-induced orexigenic effects (Fig. 6F-G). Hence, we further tested the role of L-type calcium channel in orexin-A stimulated feeding behavior. Nifedipine exhibited little effect on food intake, but inhibited orexin-A stimulated feeding behavior (Fig. 6H). Orexin-A has also been reported to be involved in the regulation of fasting-induced hyperphagia. As shown in Fig. 6I, i.c.v administration of nifedipine (50 $\mu$ g/kg) significantly alleviated the increase in food intake induced by fasting. These results suggest that the calcium-dependent hypothalamic AMPK activation especially by L-type calcium channel, contributes to the orexigenic effects induced by orexin-A.

## Discussion

In the present study, we provide evidence for the first time that hypothalamic L-type calcium channel mediates orexin-A-induced calcium-dependent AMPK activation, which may be involved in orexin-A-induced orexigenic effects. Considering the current knowledge on the signaling pathways underlying orexin-mediated effects and on the role of AMPK in food intake, our study connects the dots of understanding of the known effect of orexin-A.

Orexin-A is released from orexin-producing neurons that localize in the LHA in response to fasting and causes hyperphagia (Baird et al., 2009). Orexin-A-stimulated

MOL#86744

hyperphagia plays an important role in the abnormal control of eating behavior in the patients with eating-disorders ( Baranowska et al., 2008; Bronsky et al., 2011; Steffen et al., 2006). However, the precise molecular mechanism underlying orexin-A-stimulated eating behavior remains yet largely unknown. Many anorexic and orexigenic molecules alter AMPK activity and produce effects on energy metabolism, including leptin,  $\alpha$ -lipoic acid , fatty acid synthase inhibitor (C75) , adiponectin, ghrelin and cannabinoids (Kim et al., 2004a; Kim et al., 2004b; Kola et al., 2005; Kubota et al., 2007; Lopez et al., 2008; Minokoshi et al., 2002; Wen et al., 2010). Our present study firstly demonstrated that orexin-A increased hypothalamic AMPK activity. Two AMPK inhibitors can prevent the orexigenic effect of orexin-A, indicating that orexin-A exerts orexigenic action via AMPK signaling pathway. AMPK can activate NPY neurons in the hypothalamic ARC to increase food intake and increase NPY synthesis (Kohno et al., 2011). In our current study, orexin-A up-regulated the total NPY content, which was consisted with previous study (Martins et al., 2010). This effect was blocked by AMPK inhibitor compound C, indicating a positive correlation of AMPK activity and NPY neurons activity. Taken together, our present study demonstrates that orexin-A-induced feeding behavior at least largely arrives from AMPK activation. Considering the non-specificity of chemical inhibitors, genetic approach to conditionally knockdown AMPK in NPY neurons should be used in the future.

Numerous studies indicate that the tumor suppressor protein LKB1 and the cellular AMP/ATP ratio are responsible for the activation of AMPK in pathological conditions, including hypoxia and glucose deprivation (Kemp et al., 1999). In the present study, we found that orexin-A had little influence on LKB1 phosphorylation. No changes of AMP/ATP ratio in the hypothalamus was observed in our experimental setting. Recently, CaMKK $\beta$  is shown to function as an established AMPK upstream kinase. CaMKK $\beta$  can regulate the phosphorylation of AMPK in NPY neurons of hypothalamus independent of AMP/ATP ratio (Anderson et al., 2008; Bair et al., 2009; Fogarty et al., 2010). These findings highlight that  $\text{Ca}^{2+}/\text{CaM/CaMKK}\beta$  pathway may

MOL#86744

act as a coupler linking metabolic hormone to the phosphorylation of AMPK. I.c.v injection of STO609, an widely-used inhibitor of CaMKK $\beta$  (Anderson et al., 2008; Pfisterer et al., 2011; Tokumitsu et al., 2003), attenuated AMPK activation induced by orexin-A in hypothalamic ARC. We also confirmed the role of Ca $^{2+}$ /CaM/CaMKK $\beta$  pathway in cultured hypothalamic neurons. Pre-incubation with intracellular calcium chelator BAPTA-AM almost completely blocked orexin-A-induced AMPK activation in cultured hypothalamic neurons. In Ca $^{2+}$ -free medium, orexin-A-stimulated AMPK activation was also inhibited. These results demonstrate that orexin-A activates AMPK activation via Ca $^{2+}$ /CaM/CaMKK $\beta$  pathway. The role of CaMKK $\beta$  pathway in the orexigenic effect of orexin-A requires further investigation using genetic approaches.

It has been demonstrated that activation of VGCCs mediates orexin-A-activated Ca $^{2+}$  entry in native neurons (Kohlmeier et al., 2008; Uramura et al., 2001; Xu et al., 2002). Our present study showed that L-type calcium channel blocker nifedipine significantly inhibited the increase in I<sub>HVA</sub> induced by orexin-A in NPY neurons. Nifedipine also significantly inhibited orexin-A-induced AMPK phosphorylation in cultured hypothalamic neurons. Considering that there are some differences between cultured hypothalamic neurons from ARC of neonatal rats and adult animals, we further investigated whether acitvation of L-type calcium channel mediates orexin-A-induced AMPK activation *in vivo*. I.c.v injection of nifedipine significantly prevented orexin-A and fasting-induced feeding behavior. Taken together, these results strongly support our hypothesis that activation of L-type calcium channel is largely responsible for hypothalamic AMPK activation and may affect orexin-A-induced orexigenic effects. Recently, it has been reported that antagonism of T-type calcium channel inhibits high-fat diet-induced weight gain in mice (Uebele et al., 2009). Hence, we speculate that L-type calcium channel is another potential drug target for the treatment of metabolic diseases.

To understand the mechanism of orexin-A on L-type calcium channel, PLC inhibitor U73122 and PKC inhibitor GF109203X was used to investigate. U73122 significantly inhibited the increase in I<sub>HVA</sub> produced by orexin-A. Furthermore, U73122 attenuated

orexin-A-induced hypothalamic AMPK activation and orexigenic effects. These results suggest that OXR1-PLC signaling pathway is required for orexin-A's effect. Previous studies have indicated that U73122 exerts several additional effects, including blockade of L-type  $\text{Ca}^{2+}$  channels and a direct activation of PLC (Klein et al., 2011; Taylor and Broad, 1998). In our current study, little direct effects of U73122 on VGCCs currents were observed. As a key downstream of PLC, PKC mediated orexin-A's effect on calcium channel. A PKC inhibitor, GF109203X, abolished orexin-A-induced increase in calcium current, which was consistent with previous studies on different neurons (Uramura K et al., 2001; Kohlmeier et al., 2008; Xia et al., 2009). PKC activation could lead L-type calcium channels phosphorylation and make channels be activated easily (Li D et al., 2005). However, the regulation of L-type calcium channels by PKC activation is complex, with both stimulation and inhibition of Ca current being observed (Kamp TJ et al., 2000). We found both Cav1.2 and Cav1.3 expressed in ARC neurons using PCR technology (seen in supplementary Fig4). It remains to be determined whether any individual phosphorylation site of Cav1.2 or Cav1.3 by PKC will contribute to orexin-A's effect. Further investigation will be performed in our next study.

It should be noted that besides VGCCs, there may exist other calcium entry routes involved in the effect of orexin-A. Transient receptor potential channels (TRPCs) blocker SKF96365 (25 nmol) attenuated, but not prevented orexin-A-induced activation of hypothalamic AMPK (seen in supplementary Fig5), indicating that TRPCs, which are activated by orexin-A (Cvetkovic-Lopes et al., 2010; Larsson et al., 2005; Peltonen et al., 2009), may contribute to orexin-A's effect. In our preliminary experiment, we found that low concentration of orexin-A (1 nM) seemed to exhibit little effect on AMPK activation, although it can increase calcium current. We found that calcium influx through VGCCs was predominant in orexin-A-induced AMPK activation, while  $\text{Ca}^{2+}$  release from intracellular store and other calcium entry routes were also involved in this effect. Thus, we speculated that orexin-A-induced  $\text{Ca}^{2+}$  current was the initiation factor to activate other calcium entry routes. Low concentration of orexin-A failed to increase AMPK phosphorylation, which may be

MOL#86744

due to its weak action on  $\text{Ca}^{2+}$  current that cannot produce enough calcium signal to activate secondary cascade reaction, including calcium-dependent calcium release and calcium-dependent calcium influx.

Our electrophysiological results revealed that orexin-A increased the frequency of action potentials and caused membrane depolarization in hypothalamic NPY neurons (seen in supplementary Fig3). How L-type channel potentiation affects the firing properties of NPY neurons is a very interesting question. NPY neurons are sensitive to energy status and previous studies have revealed that AMPK activity controls excitation of NPY/AgRP neurons (Kohno D et al., 2011; Murphy BA et al., 2009; Mountjoy PD et al., 2007). We hypothesize that L-type channel potentiation increased the frequency of action potentials via activating AMPK. On the other hand, it can be speculated that increased action potential frequency can open more VGCCs. Some studies have also revealed that AMPK activation increases  $[\text{Ca}^{2+}]_{\text{i}}$  in NPY neurons (Kohno D et al., 2008; Kohno D et al., 2011) but little is known about mechanism. A synaptic AMPK-dependent positive feedback loop was involved in the hunger states sensing (Yang Y et al, 2011). A positive loop including “VGCCs– $[\text{Ca}^{2+}]_{\text{i}}$  -AMPK-Neuron Excitation-VGCCs” may also exist. However, it requires more evidence.

In conclusion, our results demonstrated that the upregulation of L-type calcium channel by orexin-A via OX<sub>1</sub>R-PLC-PKC signaling pathway played a central role in the orexin-A-induced activation of hypothalamic AMPK in NPY neurons (Fig.7). Considering that L-type calcium channel blockers have been used widely in clinical practice, our studies provide a potential new strategy for treatment of abnormal eating behavior such as binge-eating and purging behavior.

MOL#86744

## Authorship Contributions

Participated in research design: WN Wu, PF Wu, F Wang and JG Chen

Conducted experiments: WN Wu, J Zhou, PF Wu, XL Guan, Z Zhang, YJ Yang, LH Long, N Xie

Performed data analysis: WN Wu, PF Wu

Wrote or contributed to the writing of the manuscript: WN Wu, PF Wu, F Wang and JG Chen

## References

- Anderson KA, Ribar TJ, Lin F, Noeldner PK, Green MF, Muehlbauer MJ, Witters LA, Kemp BE and Means AR (2008) Hypothalamic CaMKK2 contributes to the regulation of energy balance. *Cell Metab* **7**(5):377-388.
- Bair AM, Thippegowda PB, Freichel M, Cheng N, Ye RD, Vogel SM, Yu Y, Flockerzi V, Malik AB and Tiruppathi C (2009) Ca<sup>2+</sup> entry via TRPC channels is necessary for thrombin-induced NF-kappaB activation in endothelial cells through AMP-activated protein kinase and protein kinase C $\delta$ . *J Biol Chem* **284**(1):563-574.
- Baird JP, Choe A, Loveland JL, Beck J, Mahoney CE, Lord JS and Grigg LA (2009) Orexin-A hyperphagia: hindbrain participation in consummatory feeding responses. *Endocrinology* **150**(3):1202-1216.
- Baranowska B, Baranowska-Bik A, Bik W and Martynska L (2008) The role of leptin and orexins in the dysfunction of hypothalamo-pituitary-gonadal regulation and in the mechanism of hyperactivity in patients with anorexia nervosa. *Neuro Endocrinol Lett* **29**(1):37-40.
- Bronsky J, Nedvidkova J, Krasnicanova H, Vesela M, Schmidtova J, Koutek J, Kellermayer R, Chada M, Kabelka Z, Hrdlicka M, Nevoral J and Prusa R (2011) Changes of orexin A plasma levels in girls with anorexia nervosa during eight weeks of realimentation. *Int J Eat Disord* **44**(6):547-552.
- Coolen EJ, Arts IC, Swennen EL, Bast A, Stuart MA and Dagnelie PC (2008) Simultaneous determination of adenosine triphosphate and its metabolites in human whole blood by RP-HPLC and UV-detection. *J Chromatogr B Analyt Technol Biomed Life Sci* **864**(1-2):43-51.
- Cvetkovic-Lopes V, Eggermann E, Uschakov A, Grivel J, Bayer L, Jones BE, Serafin M and Muhlethaler M (2010) Rat hypocretin/orexin neurons are maintained in a depolarized state by TRPC channels. *PLoS One* **5**(12):e15673.
- Date Y, Ueta Y, Yamashita H, Yamaguchi H, Matsukura S, Kangawa K, Sakurai T, Yanagisawa M and Nakazato M (1999) Orexins, orexigenic hypothalamic

MOL#86744

- peptides, interact with autonomic, neuroendocrine and neuroregulatory systems.  
*Proc Natl Acad Sci U S A* **96**(2):748-753.
- de Lecea L, Kilduff TS, Peyron C, Gao X, Foye PE, Danielson PE, Fukuhara C, Battenberg EL, Gautvik VT, Bartlett FS, 2nd, Frankel WN, van den Pol AN, Bloom FE, Gautvik KM and Sutcliffe JG (1998) The hypocretins: hypothalamus-specific peptides with neuroexcitatory activity. *Proc Natl Acad Sci U S A* **95**(1):322-327.
- Dessy C and Godfraind T (1996) The effect of L-type calcium channel modulators on the mobilization of intracellular calcium stores in guinea-pig intestinal smooth muscle. *Br J Pharmacol* **119**(1):142-148.
- Dube MG, Horvath TL, Kalra PS and Kalra SP (2000) Evidence of NPY Y5 receptor involvement in food intake elicited by orexin A in sated rats. *Peptides* **21**(10):1557-1560.
- Edwards CM, Abusnana S, Sunter D, Murphy KG, Ghatei MA and Bloom SR (1999) The effect of the orexins on food intake: comparison with neuropeptide Y, melanin-concentrating hormone and galanin. *J Endocrinol* **160**(3):R7-12.
- Fogarty S, Hawley SA, Green KA, Saner N, Mustard KJ and Hardie DG (2010) Calmodulin-dependent protein kinase kinase-beta activates AMPK without forming a stable complex: synergistic effects of Ca<sup>2+</sup> and AMP. *Biochem J* **426**(1):109-118.
- Haynes AC, Jackson B, Chapman H, Tadayyon M, Johns A, Porter RA and Arch JR (2000) A selective orexin-1 receptor antagonist reduces food consumption in male and female rats. *Regul Pept* **96**(1-2):45-51.
- Horvath TL and Diano S (2004) The floating blueprint of hypothalamic feeding circuits. *Nature reviews Neuroscience* **5**(8):662-667.
- Ida T, Nakahara K, Kuroiwa T, Fukui K, Nakazato M, Murakami T and Murakami N (2000) Both corticotropin releasing factor and neuropeptide Y are involved in the effect of orexin (hypocretin) on the food intake in rats. *Neurosci Lett* **293**(2):119-122.
- Jain MR, Horvath TL, Kalra PS and Kalra SP (2000) Evidence that NPY Y1 receptors

MOL#86744

- are involved in stimulation of feeding by orexins (hypocretins) in sated rats.  
*Regul Pept* **87**(1-3):19-24.
- Kemp BE, Mitchelhill KI, Stapleton D, Michell BJ, Chen ZP and Witters LA (1999)  
Dealing with energy demand: the AMP-activated protein kinase. *Trends Biochem Sci* **24**(1):22-25.
- Kim EK, Miller I, Aja S, Landree LE, Pinn M, McFadden J, Kuhajda FP, Moran TH and Ronnett GV (2004a) C75, a fatty acid synthase inhibitor, reduces food intake via hypothalamic AMP-activated protein kinase. *J Biol Chem* **279**(19):19970-19976.
- Kim MS, Park JY, Namkoong C, Jang PG, Ryu JW, Song HS, Yun JY, Namgoong IS, Ha J, Park IS, Lee IK, Viollet B, Youn JH, Lee HK and Lee KU (2004b) Anti-obesity effects of alpha-lipoic acid mediated by suppression of hypothalamic AMP-activated protein kinase. *Nat Med* **10**(7):727-733.
- Klein RR, Bourdon DM, Costales CL, Wagner CD, White WL, Williams JD, Hicks SN, Sondek J and Thakker DR (2011) Direct activation of human phospholipase C by its well known inhibitor u73122. *J Biol Chem* **286**(14):12407-12416.
- Kohlmeier KA, Watanabe S, Tyler CJ, Burlet S and Leonard CS (2008) Dual orexin actions on dorsal raphe and laterodorsal tegmentum neurons: noisy cation current activation and selective enhancement of Ca<sup>2+</sup> transients mediated by L-type calcium channels. *J Neurophysiol* **100**(4):2265-2281.
- Kohno D, Sone H, Tanaka S, Kurita H, Gantulga D and Yada T (2011) AMP-activated protein kinase activates neuropeptide Y neurons in the hypothalamic arcuate nucleus to increase food intake in rats. *Neurosci Lett* **499**(3):194-198.
- Kola B, Hubina E, Tucci SA, Kirkham TC, Garcia EA, Mitchell SE, Williams LM, Hawley SA, Hardie DG, Grossman AB and Korbonits M (2005) Cannabinoids and ghrelin have both central and peripheral metabolic and cardiac effects via AMP-activated protein kinase. *J Biol Chem* **280**(26):25196-25201.
- Kubota N, Yano W, Kubota T, Yamauchi T, Itoh S, Kumagai H, Kozono H, Takamoto I, Okamoto S, Shiuchi T, Suzuki R, Satoh H, Tsuchida A, Moroi M, Sugi K,

MOL#86744

- Noda T, Ebinuma H, Ueta Y, Kondo T, Araki E, Ezaki O, Nagai R, Tobe K, Terauchi Y, Ueki K, Minokoshi Y and Kadokawa T (2007) Adiponectin stimulates AMP-activated protein kinase in the hypothalamus and increases food intake. *Cell Metab* **6**(1):55-68.
- Larsson KP, Peltonen HM, Bart G, Louhivuori LM, Penttonen A, Antikainen M, Kukkonen JP and Akerman KE (2005) Orexin-A-induced Ca<sup>2+</sup> entry: evidence for involvement of trpc channels and protein kinase C regulation. *J Biol Chem* **280**(3):1771-1781.
- Lin F, Xin Y, Wang J, Ma L, Liu J, Liu C, Long L, Wang F, Jin Y, Zhou J and Chen J (2007) Puerarin facilitates Ca(2+)-induced Ca(2+) release triggered by KCl-depolarization in primary cultured rat hippocampal neurons. *Eur J Pharmacol* **570**(1-3):43-49.
- Lopez M, Lage R, Saha AK, Perez-Tilve D, Vazquez MJ, Varela L, Sangiao-Alvarellos S, Tovar S, Raghay K, Rodriguez-Cuenca S, Deoliveira RM, Castaneda T, Datta R, Dong JZ, Culler M, Sleeman MW, Alvarez CV, Gallego R, Lelliott CJ, Carling D, Tschop MH, Dieguez C and Vidal-Puig A (2008) Hypothalamic fatty acid metabolism mediates the orexigenic action of ghrelin. *Cell Metab* **7**(5):389-399.
- Ma LQ, Liu C, Wang F, Xie N, Gu J, Fu H, Wang JH, Cai F, Liu J and Chen JG (2009) Activation of phosphatidylinositol-linked novel D1 dopamine receptors inhibits high-voltage-activated Ca<sup>2+</sup> currents in primary cultured striatal neurons. *J Neurophysiol* **101**(5):2230-2238.
- Martins PJ, Marques MS, Tufik S and D'Almeida V (2010) Orexin activation precedes increased NPY expression, hyperphagia, and metabolic changes in response to sleep deprivation. *Am J Physiol Endocrinol Metab* **298**(3):E726-734.
- Ming Y, Zhang H, Long L, Wang F, Chen J and Zhen X (2006) Modulation of Ca<sup>2+</sup> signals by phosphatidylinositol-linked novel D1 dopamine receptor in hippocampal neurons. *J Neurochem* **98**(4):1316-1323.
- Minokoshi Y, Kim YB, Peroni OD, Fryer LG, Muller C, Carling D and Kahn BB (2002) Leptin stimulates fatty-acid oxidation by activating AMP-activated

MOL#86744

- protein kinase. *Nature* **415**(6869):339-343.
- Myauchi A, Hruska KA, Greenfield EM, Duncan R, Alvarez J, Barattolo R, Colucci S, Zambonin-Zallone A, Teitelbaum SL and Teti A (1990) Osteoclast cytosolic calcium, regulated by voltage-gated calcium channels and extracellular calcium, controls podosome assembly and bone resorption. *J Cell Biol* **111**(6 Pt 1):2543-2552.
- Mulvaney JM, Zhang T, Fewtrell C and Roberson MS (1999) Calcium influx through L-type channels is required for selective activation of extracellular signal-regulated kinase by gonadotropin-releasing hormone. *J Biol Chem* **274**(42):29796-29804.
- Muroya S, Funahashi H, Yamanaka A, Kohno D, Uramura K, Nambu T, Shibahara M, Kuramochi M, Takigawa M, Yanagisawa M, Sakurai T, Shiota S and Yada T (2004) Orexins (hypocretins) directly interact with neuropeptide Y, POMC and glucose-responsive neurons to regulate Ca<sup>2+</sup> signaling in a reciprocal manner to leptin: orexigenic neuronal pathways in the mediobasal hypothalamus. *Eur J Neurosci* **19**(6):1524-1534.
- Murphy BA, Fioramonti X, Jochnowitz N, Fakira K, Gagen K, Contie S, Lorsignol A, Penicaud L, Martin WJ and Routh VH (2009) Fasting enhances the response of arcuate neuropeptide Y-glucose-inhibited neurons to decreased extracellular glucose. *Am J Physiol Cell Physiol* **296**(4):C746-756.
- Paxinos G, Watson CR and Emson PC (1980) AChE-stained horizontal sections of the rat brain in stereotaxic coordinates. *J Neurosci Methods* **3**(2):129-149.
- Peltonen HM, Magga JM, Bart G, Turunen PM, Antikainen MS, Kukkonen JP and Akerman KE (2009) Involvement of TRPC3 channels in calcium oscillations mediated by OX(1) orexin receptors. *Biochem Biophys Res Commun* **385**(3):408-412.
- Peti-Peterdi J and Bell PD (1999) Cytosolic [Ca<sup>2+</sup>] signaling pathway in macula densa cells. *Am J Physiol* **277**(3 Pt 2):F472-476.
- Pfisterer SG, Mauthe M, Codogno P and Proikas-Cezanne T (2011) Ca<sup>2+</sup>/calmodulin-dependent kinase (CaMK) signaling via CaMKI and

MOL#86744

- AMP-activated protein kinase contributes to the regulation of WIPI-1 at the onset of autophagy. *Mol Pharmacol* **80**(6):1066-1075.
- Pinto S, Roseberry AG, Liu H, Diano S, Shanabrough M, Cai X, Friedman JM and Horvath TL (2004) Rapid rewiring of arcuate nucleus feeding circuits by leptin. *Science* **304**(5667):110-115.
- Potter WB, O'Riordan KJ, Barnett D, Osting SM, Wagoner M, Burger C and Roopra A (2010) Metabolic regulation of neuronal plasticity by the energy sensor AMPK. *PLoS One* **5**(2):e8996.
- Rocha AA, Guerra-Sa R, Silveira NA, Anselmo-Franci JA and Franci CR (2006) Neuropeptide Y in the medial basal hypothalamus and medial preoptic area during the induction of LH surge may be controlled by locus coeruleus. *Neuropeptides* **40**(1):57-63.
- Russell RR, 3rd, Bergeron R, Shulman GI and Young LH (1999) Translocation of myocardial GLUT-4 and increased glucose uptake through activation of AMPK by AICAR. *Am J Physiol* **277**(2 Pt 2):H643-649.
- Sakurai T, Amemiya A, Ishii M, Matsuzaki I, Chemelli RM, Tanaka H, Williams SC, Richardson JA, Kozlowski GP, Wilson S, Arch JR, Buckingham RE, Haynes AG, Carr SA, Annan RS, McNulty DE, Liu WS, Terrell JA, Elshourbagy NA, Bergsma DJ and Yanagisawa M (1998) Orexins and orexin receptors: a family of hypothalamic neuropeptides and G protein-coupled receptors that regulate feeding behavior. *Cell* **92**(4):573-585.
- Steffen KJ, Roerig JL, Mitchell JE and Uppala S (2006) Emerging drugs for eating disorder treatment. *Expert Opin Emerg Drugs* **11**(2):315-336.
- Taylor CW and Broad LM (1998) Pharmacological analysis of intracellular Ca<sup>2+</sup> signalling: problems and pitfalls. *Trends Pharmacol Sci* **19**(9):370-375.
- Tokumitsu H, Inuzuka H, Ishikawa Y and Kobayashi R (2003) A single amino acid difference between alpha and beta Ca<sup>2+</sup>/calmodulin-dependent protein kinase kinase dictates sensitivity to the specific inhibitor, STO-609. *J Biol Chem* **278**(13):10908-10913.
- Uebel VN, Gotter AL, Nuss CE, Kraus RL, Doran SM, Garson SL, Reiss DR, Li Y,

MOL#86744

- Barrow JC, Reger TS, Yang ZQ, Ballard JE, Tang C, Metzger JM, Wang SP, Koblan KS and Renger JJ (2009) Antagonism of T-type calcium channels inhibits high-fat diet-induced weight gain in mice. *J Clin Invest* **119**(6):1659-1667.
- Uramura K, Funahashi H, Muroya S, Shioda S, Takigawa M and Yada T (2001) Orexin-a activates phospholipase C- and protein kinase C-mediated Ca<sup>2+</sup> signaling in dopamine neurons of the ventral tegmental area. *Neuroreport* **12**(9):1885-1889.
- Wang JH, Wang F, Yang MJ, Yu DF, Wu WN, Liu J, Ma LQ, Cai F and Chen JG (2008) Leptin regulated calcium channels of neuropeptide Y and proopiomelanocortin neurons by activation of different signal pathways. *Neuroscience* **156**(1):89-98.
- Wen JP, Liu CE, Hu YT, Chen G and Lin LX (2010) Globular adiponectin regulates energy homeostasis through AMP-activated protein kinase-acetyl-CoA carboxylase (AMPK/ACC) pathway in the hypothalamus. *Mol Cell Biochem* **344**(1-2):109-115.
- Wu X, Motoshima H, Mahadev K, Stalker TJ, Scalia R and Goldstein BJ (2003) Involvement of AMP-activated protein kinase in glucose uptake stimulated by the globular domain of adiponectin in primary rat adipocytes. *Diabetes* **52**(6):1355-1363.
- Xu R, Wang Q, Yan M, Hernandez M, Gong C, Boon WC, Murata Y, Ueta Y and Chen C (2002) Orexin-A augments voltage-gated Ca<sup>2+</sup> currents and synergistically increases growth hormone (GH) secretion with GH-releasing hormone in primary cultured ovine somatotropes. *Endocrinology* **143**(12):4609-4619.
- Yamada H, Okumura T, Motomura W, Kobayashi Y and Kohgo Y (2000) Inhibition of food intake by central injection of anti-orexin antibody in fasted rats. *Biochem Biophys Res Commun* **267**(2):527-531.
- Yamanaka A, Kunii K, Nambu T, Tsujino N, Sakai A, Matsuzaki I, Miwa Y, Goto K and Sakurai T (2000) Orexin-induced food intake involves neuropeptide Y

MOL#86744

pathway. *Brain Res* **859**(2):404-409.

Yang MJ, Wang F, Wang JH, Wu WN, Hu ZL, Cheng J, Yu DF, Long LH, Fu H, Xie N and Chen JG (2010) PI3K integrates the effects of insulin and leptin on large-conductance Ca<sup>2+</sup>-activated K<sup>+</sup> channels in neuropeptide Y neurons of the hypothalamic arcuate nucleus. *Am J Physiol Endocrinol Metab* **298**(2):E193-201.

Yang Y, Atasoy D, Su HH and Sternson SM (2011) Hunger states switch a flip-flop memory circuit via a synaptic AMPK-dependent positive feedback loop. *Cell* **146**(6):992-1003.

MOL#86744

## Footnotes

Wen-Ning Wu, Peng-Fei Wu and Jun Zhou contributed equally to this work

This work was supported by grants from the National Natural Science Foundation of China (NSFC, No.81222048) to *F.W*, the National Basic Research Program of China (973 Program, No. 2013CB531303), the Key Project of NSFC (No. 30930104) and the International Science & Technology Cooperation Program of China (No. 2011DFA32670) to *J.G.C.*

MOL#86744

## Figure legends

**Fig. 1.** Orexin-A activates AMPK in the hypothalamic ARC in vivo. (A) Representative immunoreactive bands and statistical results from six independent experiments show an increase in phosphorylated AMPK in ARC after i.c.v. injection of orexin-A. (B) Statistical results from six independent experiments show no change of AMP/ATP ratio in ARC after i.c.v. injection of orexin-A. (C) Representative immunoreactive bands and statistical results from four independent experiments show no change of phosphorylated LKB1 in ARC after i.c.v. injection of orexin-A. (D) Representative immunoreactive bands and statistical results from six independent experiments showing orexin-A induced AMPK activation was inhibited by CaMKK $\beta$  inhibitor STO609. Data are expressed as means  $\pm$  S.E.M.  $^{\#}p<0.05$  vs control and  $*p<0.05$  vs orexin-A.

**Fig. 2.** Orexin-A induces AMPK activation via extracellular calcium-dependent pathway in cultured rat hypothalamic ARC neurons. (A) Representative immunoreactive bands and statistical results from six independent experiments show an increase in phosphorylated AMPK in cultured rat ARC neurons after treatment with orexin-A. (B) Representative immunoreactive bands and statistical results from six independent experiments showing BAPTA-AM had no effects on AMPK activation, but it inhibited orexin-A-induced AMPK activation in the ARC neurons. (C) Representative immunoreactive bands and statistical analysis from six independent experiments showing a slow  $\text{Ca}^{2+}$  chelator EGTA had no effects on AMPK activation, but it abolished orexin-A-induced AMPK activation in the ARC neurons. (D) Representative immunoreactive bands and statistical analysis from six independent experiments showing an inhibitor of sarcoplasmic reticulum  $\text{Ca}^{2+}$  ATPase (SERCA), TG had no effects on AMPK activation, but it partially attenuated orexin-A-induced AMPK activation in the ARC neurons. (E) Representative traces and statistical results showing orexin-A increased  $[\text{Ca}^{2+}]_i$  in ARC neurons ( $n=10$ ). (F) Representative traces and statistical results showing orexin-A failed to elevate  $[\text{Ca}^{2+}]_i$

MOL#86744

in ARC neurons after replacement with  $\text{Ca}^{2+}$ -free medium (n=12). Data are expressed as means  $\pm$  S.E.M.  $^{\#}$ p<0.05 vs control or TG, and \*p<0.05 vs orexin-A.

**Fig. 3.** Orexin-A increases  $I_{\text{HVA}}$  in cultured rat NPY neurons of ARC. (A) Immunocytochemical identification of NPY neurons in cultured ARC neurons. (B) The cell in which  $I_{\text{HVA}}$  was increased by orexin-A was subsequently proved to be immunoreactive for NPY (arrow). Scale bar=20 $\mu\text{m}$ . (C) Representative traces showing orexin-A increased  $I_{\text{HVA}}$  of hypothalamic NPY neurons. (D) Dose-response curve showing orexin-A increased  $I_{\text{HVA}}$  of hypothalamic NPY neurons. (E) Time-course curve before, during and after 1 nM orexin-A treatment corresponding to Fig.3C. (F) I-V curve of  $I_{\text{HVA}}$  in hypothalamic NPY neurons. (G) Representative traces showing orexin-A shifted positively the steady-state activation curve of  $I_{\text{HVA}}$  in hypothalamic NPY neurons. (H) Representative traces showing orexin-A did not affect the inactivation kinetics of  $I_{\text{HVA}}$  in NPY neurons. The normalized conductance is plotted against the membrane potential and fitted with the Boltzmann equation. Each point represents the mean  $\pm$  S.E.M of 6 neurons.

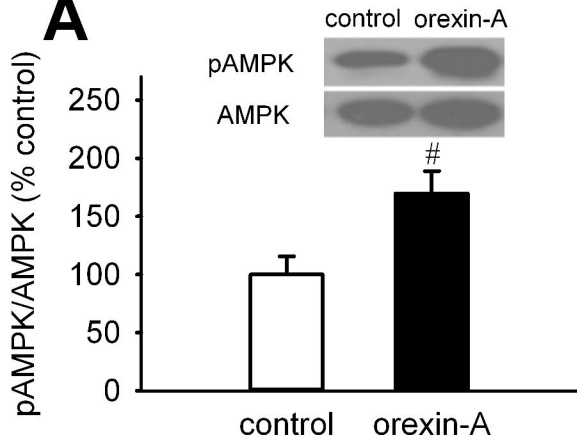
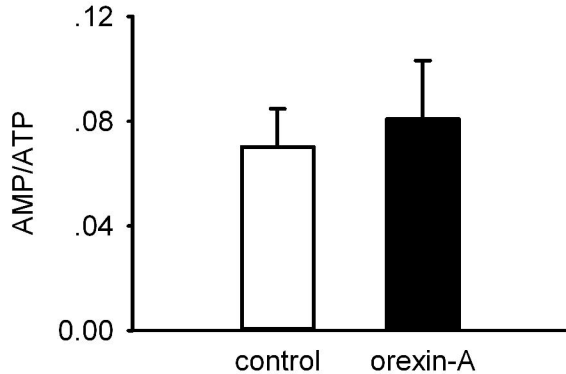
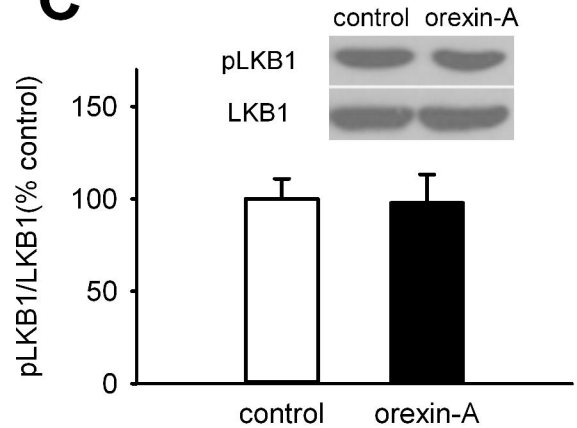
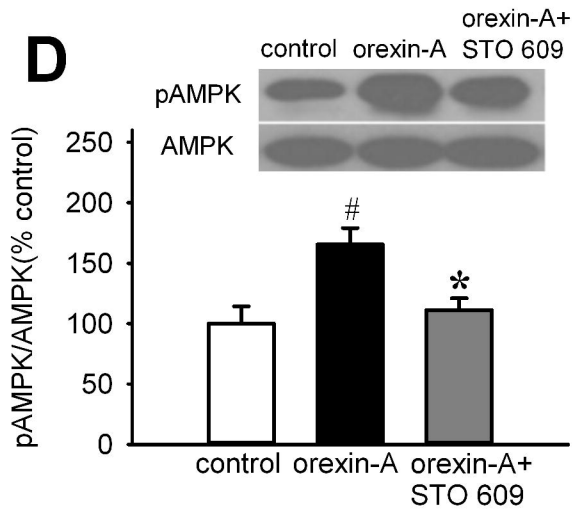
**Fig. 4.** Orexin-A increases  $I_{\text{HVA}}$  via L-type calcium channel and OX1R-PLC-PKC signaling pathway. (A-C) Representative recording and statistical analysis showing the increase in  $I_{\text{HVA}}$  induced by orexin-A was inhibited by L-type calcium channel inhibitor nifedipine (A), but not N-type calcium channel blocker  $\omega$ -conotoxin GVIA (B) and P/Q-type calcium channel blocker  $\omega$ -agatoxin TK (C). Each bar represents the mean  $\pm$  S.E.M (n=6,  $^{\#}$ p<0.05 vs control and \*p<0.05 vs  $\omega$ -conotoxin GVIA or  $\omega$ -agatoxin TK). (D-F) Representative recording and statistical analysis showing OX<sub>1</sub>R antagonist SB334867, PLC inhibitor U73122 and PKC inhibitor GF109203X had no effects on  $I_{\text{HVA}}$  in NPY neurons of ARC (n=4), but they inhibited the increase in  $I_{\text{HVA}}$  induced by orexin-A (n=6). Each bar represents the mean  $\pm$  SEM.  $^{\#}$ p<0.05 vs control and \*p<0.05 vs orexin-A. All the calibrations are the same as that in Fig. 4A.

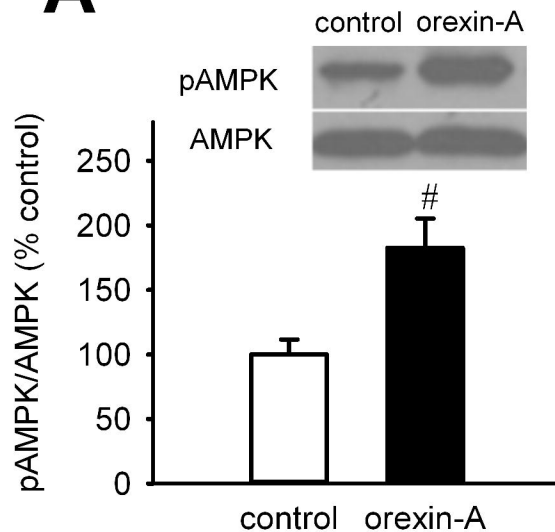
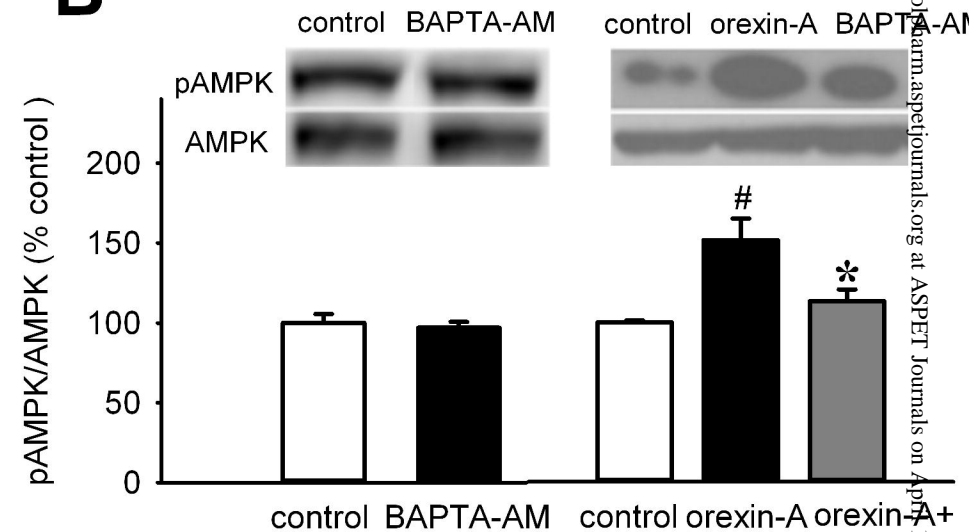
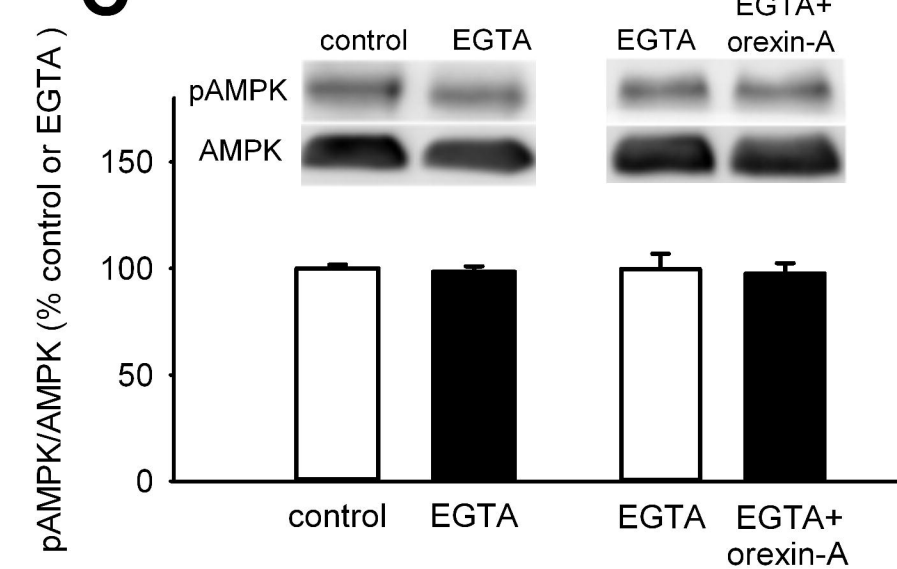
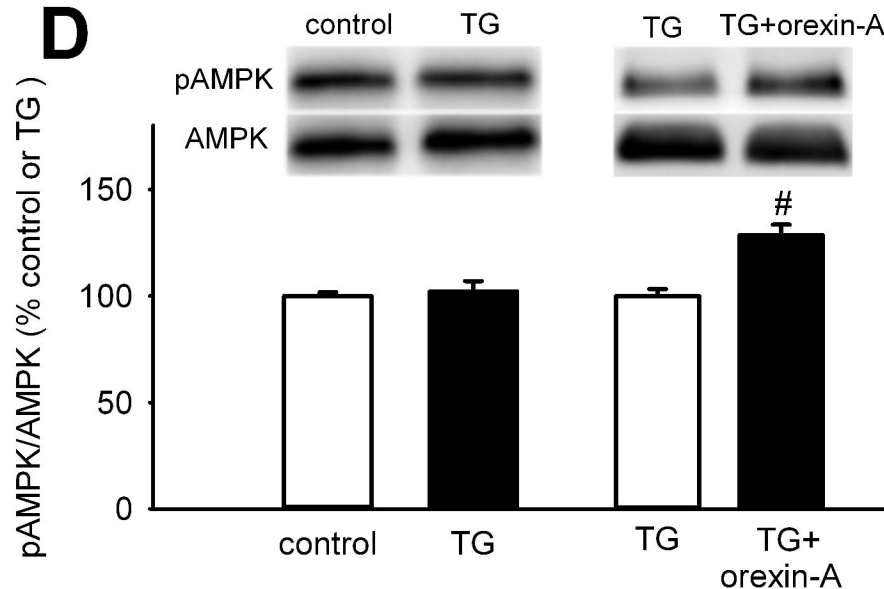
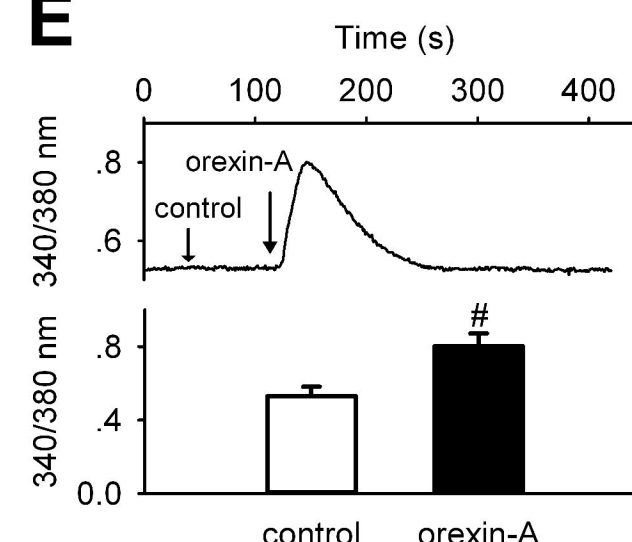
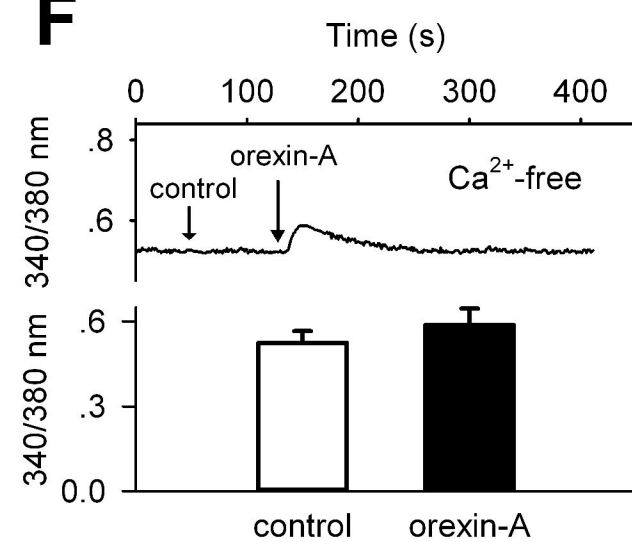
**Fig. 5.** L-type calcium channels contribute to orexin-A-induced hypothalamic AMPK activation. (A) Representative immunoreactive bands and statistical analysis from five independent experiments showing BayK8644 increased the phosphorylation of AMPK in cultured ARC neurons. This effect was inhibited by STO609. (B) Representative immunoreactive bands and statistical analysis from four independent experiments showing nifedipine inhibited AMPK activation induced by orexin-A in cultured ARC neurons. (C-D) Representative immunoreactive bands and statistical analysis from six independent experiments showing i.c.v. administration of orexin-A induced hypothalamic AMPK activation was inhibited by nifedipine (C) and PLC inhibitor U73122 (D). Data are expressed as means  $\pm$  S.E.M.  $^{\#}p<0.05$  vs control and  $*p<0.05$  vs orexin-A or BayK8644.

**Fig. 6.** Blockade of calcium-dependent AMPK activation inhibits orexin-A-induced increase in NPY content and food intake. (A-C) Statistical results from six independent experiments showing the increase in NPY content induced by orexin-A was inhibited by AMPK inhibitor compound C, CaMKK $\beta$  inhibitor STO609 and nifedipine. (D-H) Statistical analysis showing orexin-A-stimulated feeding behavior was attenuated by AMPK inhibitor compound C and ara-A, CaMKK $\beta$  inhibitor STO609, PLC inhibitor U73122 and nifedipine. (I) Statistical analysis showing nifedipine inhibited the increase in food intake induced by fasting. n=6. Data are expressed as means  $\pm$  S.E.M.  $^{\#}p<0.05$  vs vehicle and  $*p<0.05$  vs orexin-A or fasting at the same time point.

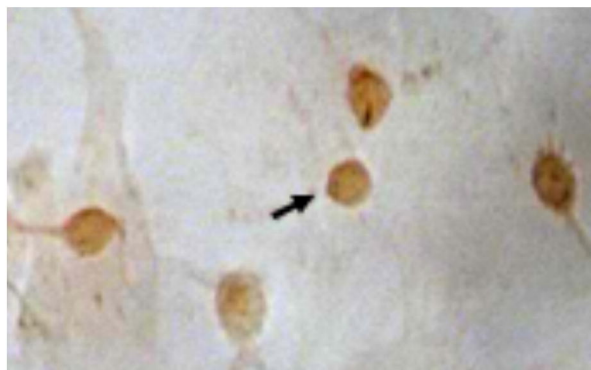
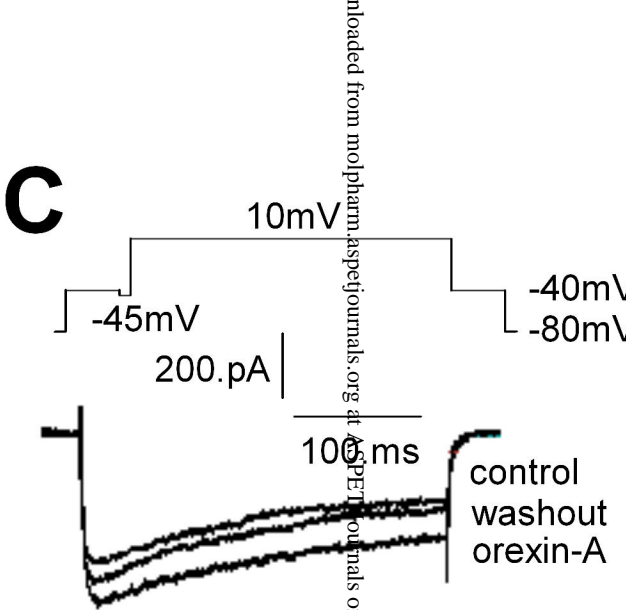
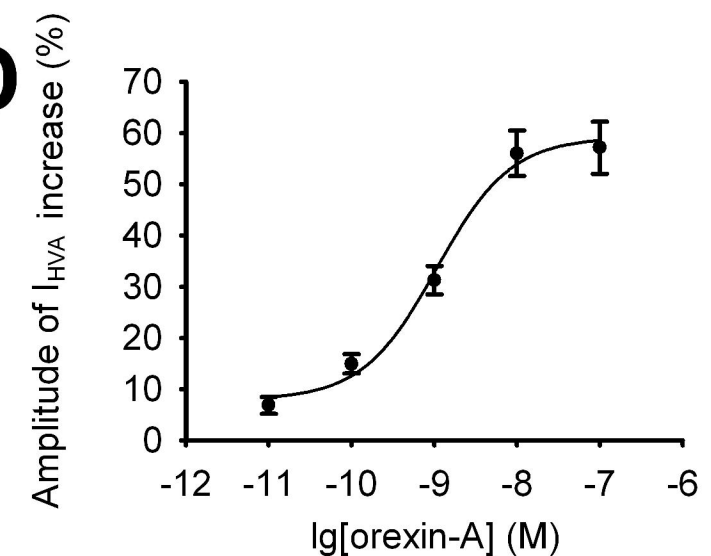
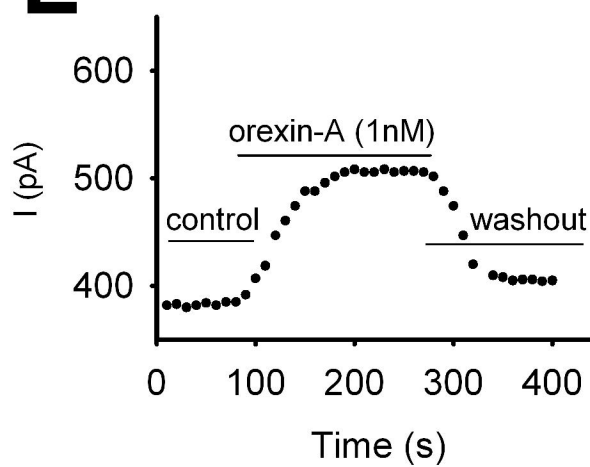
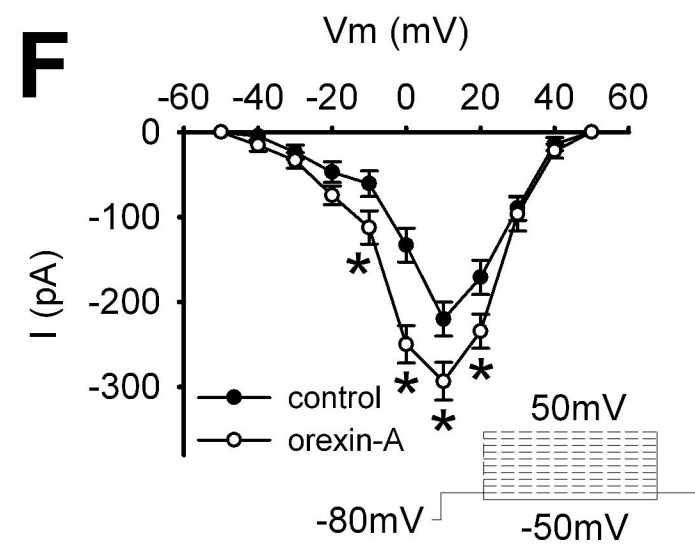
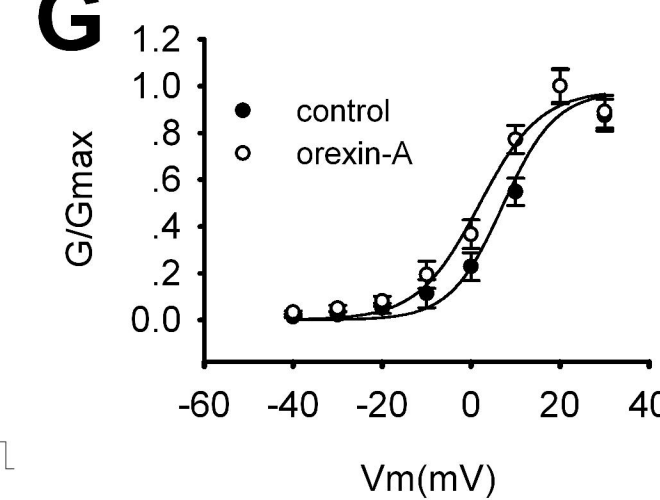
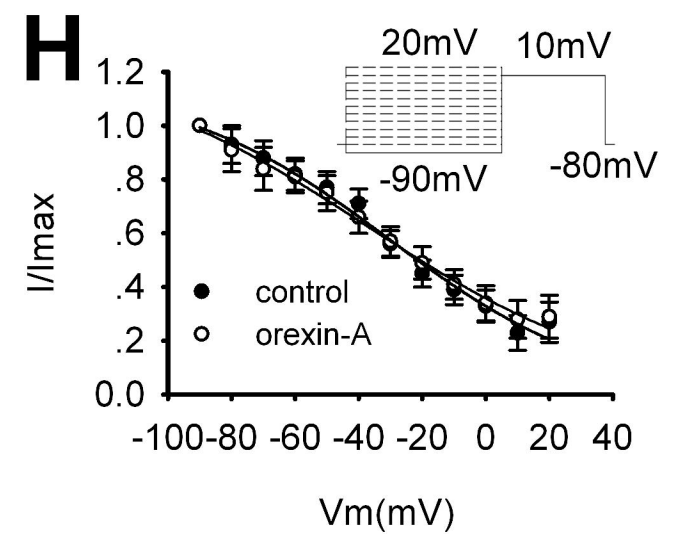
**Fig. 7.** Signaling transduction pathways mediating orexin-A's orexigenic effect on hypothalamic ARC neurons: The binding of orexin-A to the orexin receptor(s) stimulates PLC in NPY neurons and induces the activation of PKC. The activation of PKC results in the increase in  $\text{Ca}^{2+}$  currents and  $[\text{Ca}^{2+}]_i$ , thus, induces the activation of CaMKK $\beta$ , followed by activation of AMPK. The activation of AMPK results in the increase in NPY content and food intake.

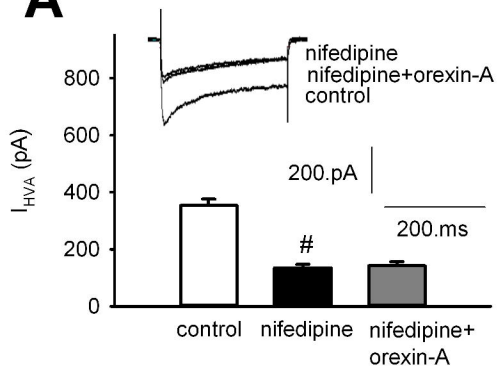
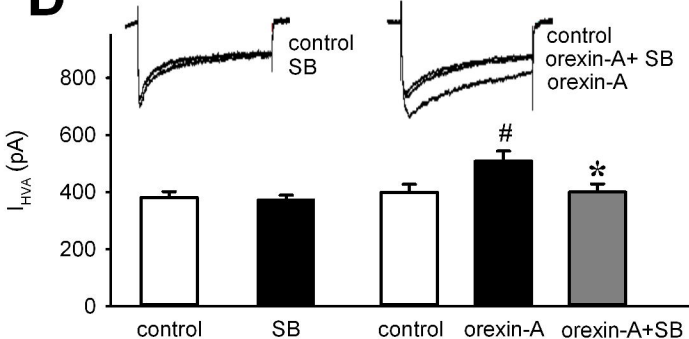
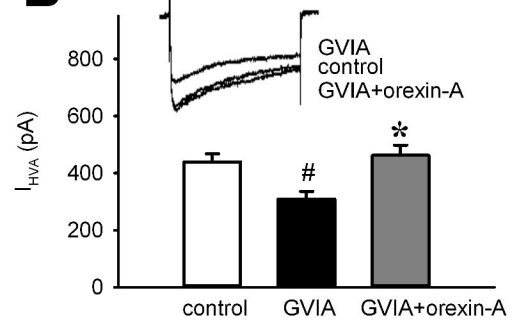
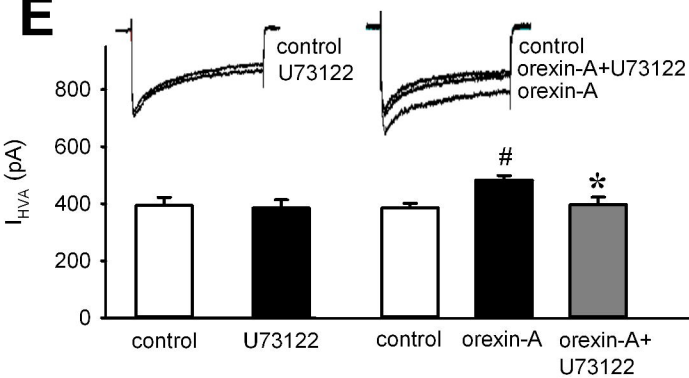
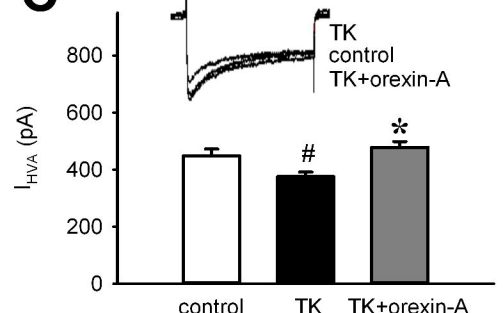
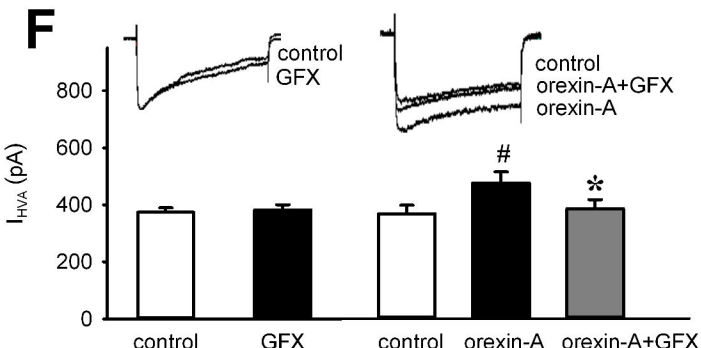
# Fig1

**A****B****C****D**

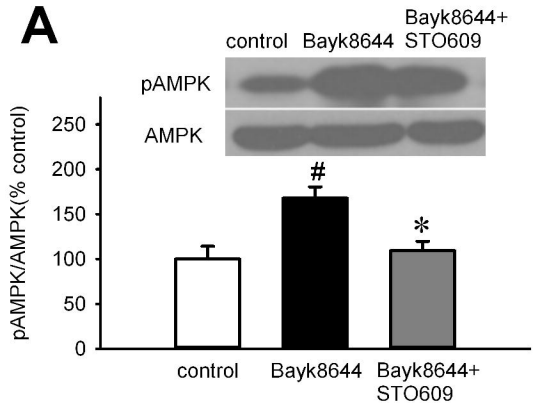
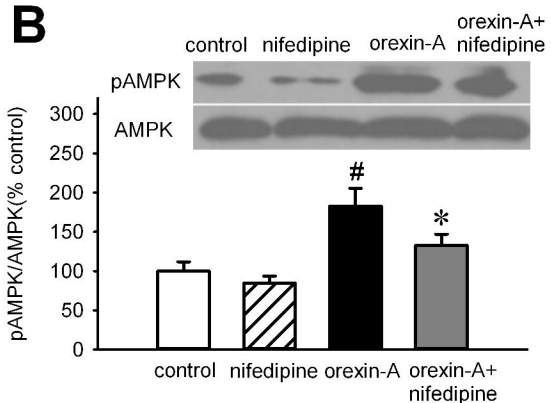
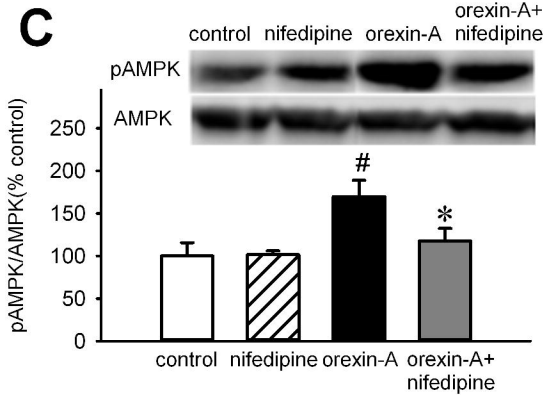
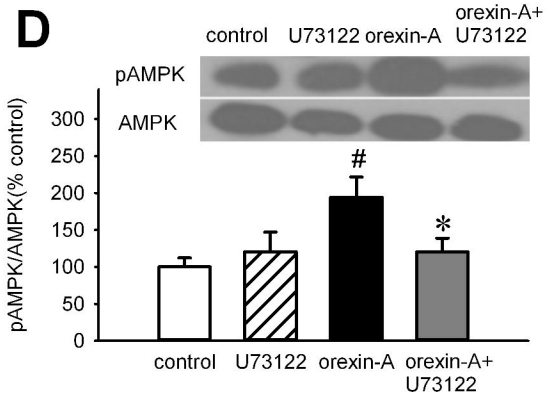
**Fig2****A****B****C****D****E****F**

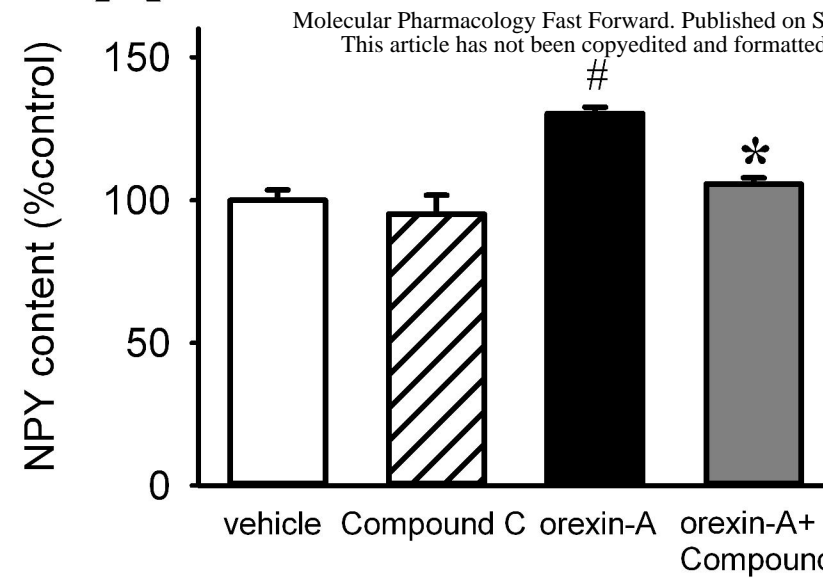
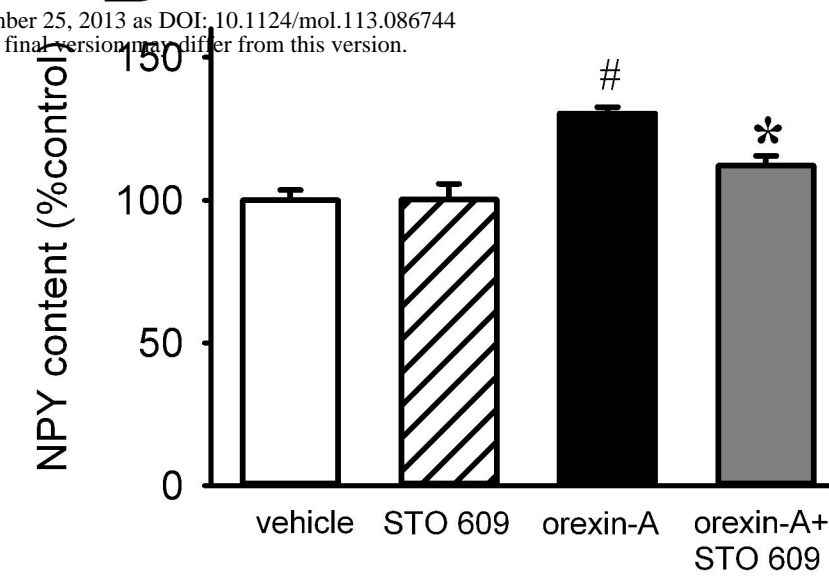
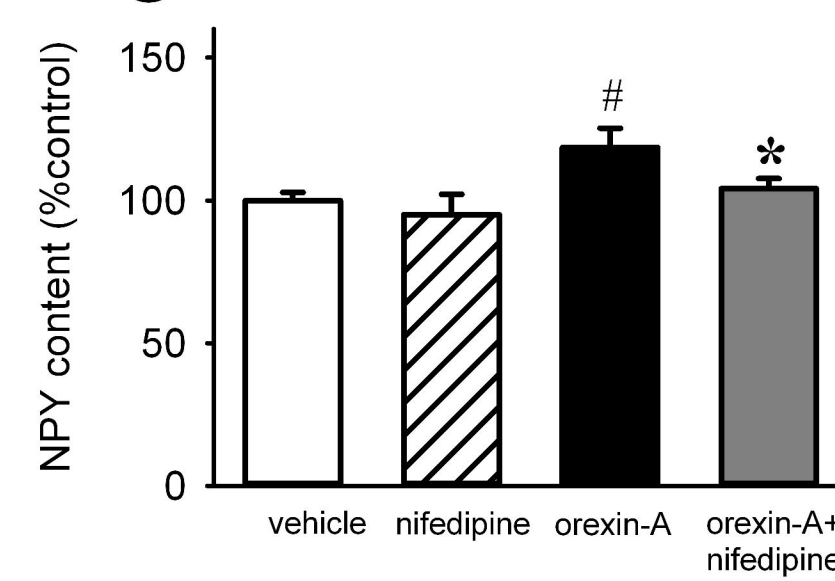
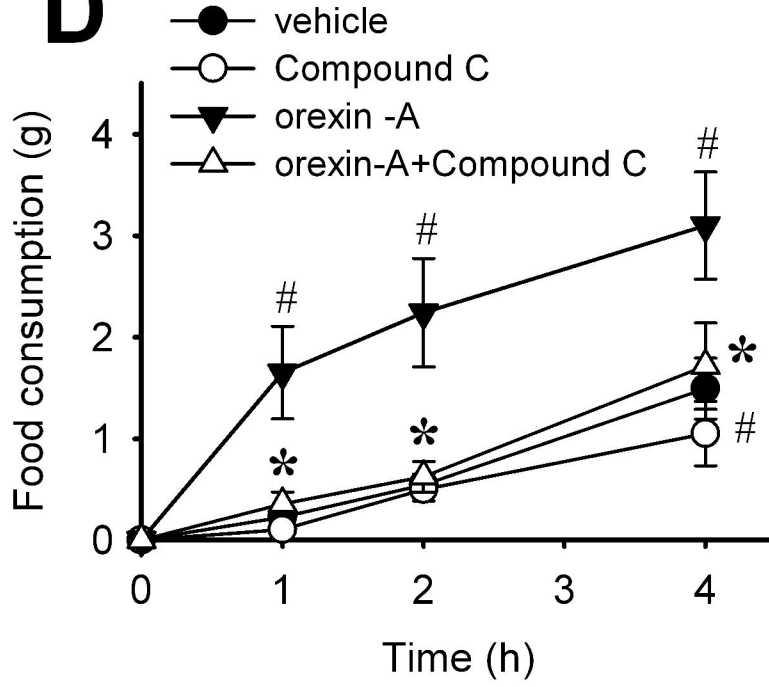
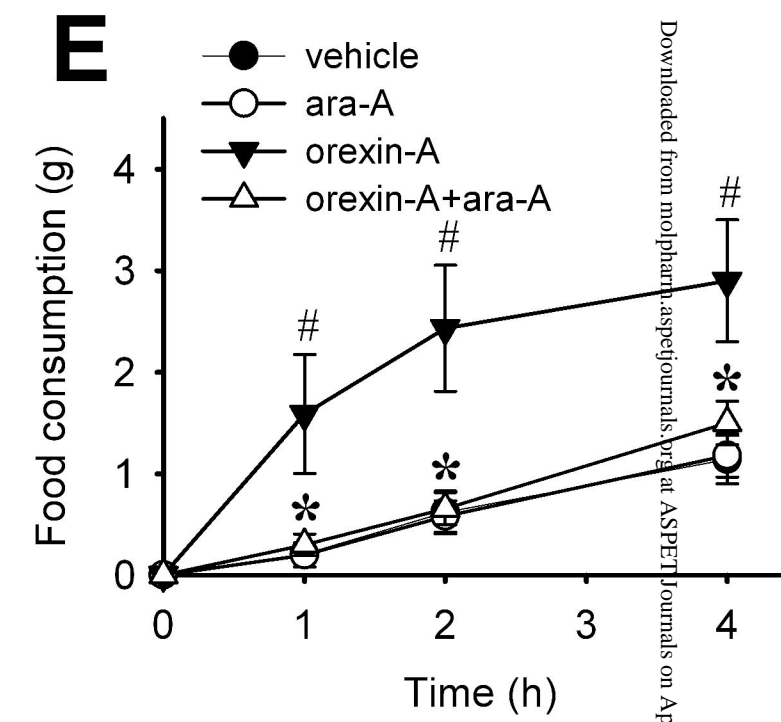
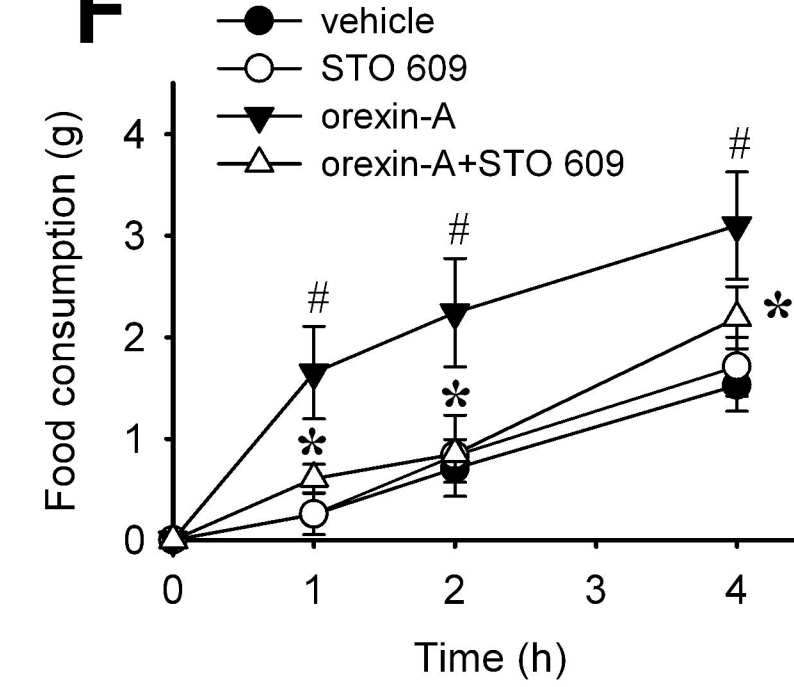
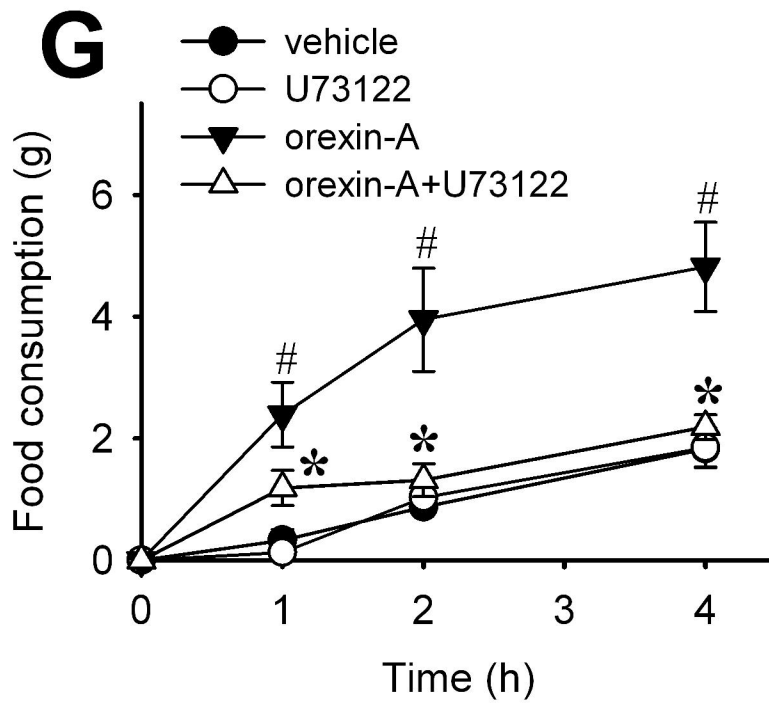
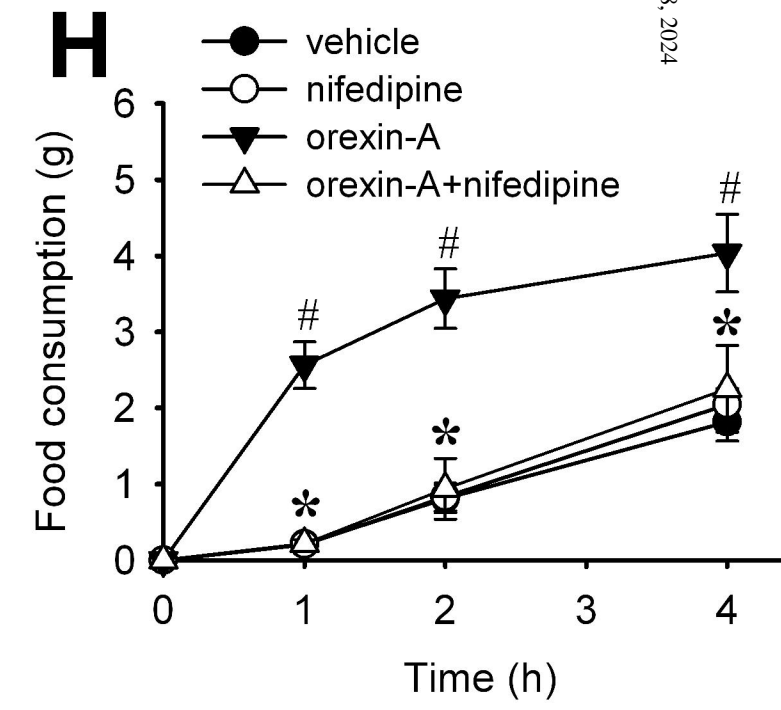
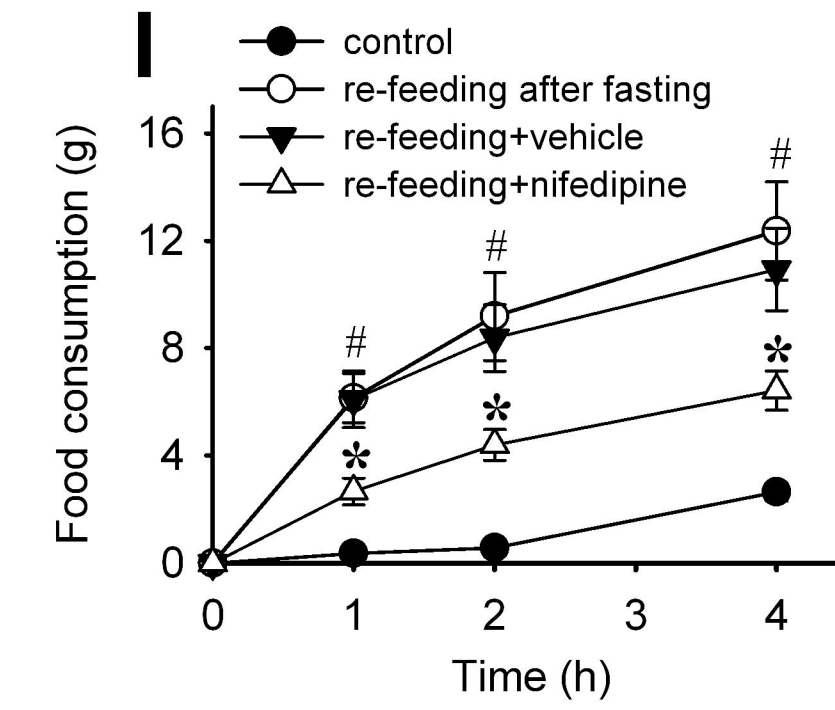
# Fig3

**A****B****C****D****E****F****G****H**

**Fig4****A****D****B****E****C****F**

# Fig5

**A****B****C****D**

**Fig6****A****B****C****D****E****F****G****H****I**

# Fig7

